Report No. 103

A SIMPLE PERFORMANCE THEORY FOR LIGHT DISPLACEMENT MULTIHULL SAILBOATS

by

W. S. Bradfield

January 1968

A SIMPLE PERFORMANCE THEORY FOR LIGHT DISPLACEMENT MULTIHULL SAILBOATS

BY

W. S. Bradfield

Department of Mechanics
State University of New York At Stony Brook

Report No. 103

January, 1968

A SIMPLE PERFORMANCE THEORY FOR LIGHT DISPLACEMENT MULTIHULL SAILBOATS

By

W. S. Bradfield

Abstract

A simple general theory for the prediction of sailboat performance in calm waters is proposed. Three parameters are shown to completely characterize the performance potential of boats fitting within the framework of the approximations made in obtaining the theory.

For handicapping, the theory is useful in predicting the performance of boats of different sizes, weights and rigs within the general category which it describes. For design purposes it will serve to predict the comparative performance of different configurations of the same boat. An example of that application is worked out in this report. The stated limitations of the theory point up the necessity for obtaining experimental information in several areas in order to determine the limits of application of the theory. Reference to one such experiment is given in the present report.

NOMENCLATURE

A - area;
AR - aspect ratio... $AR \equiv b^2/A$;
$\mathcal{A}$ - angular momentum;
C - coefficient (force), $F/\frac{\rho V^2 A}{2}$;
D - dragforce;
F - force;
L - lift;
$\mathcal{M}$ - mass (total including virtual mass) accelerated;
M - moments about the center of gravity;
R - resultant force;
S - side force perpendicular to aero-or-hydrodynamic velocity vector;
T - thrust, the component of aerodynamic force parallel to $\underset{\sim}{V}_b$;
V - velocity;
W - weight;
b - span of aero-or-hydrofoil;
c - chord of aerofoil or hydrofoil;
e - efficiency factor;
k - the hydrodynamic drag ratio $[D_f + D_o + D_w]/D_f$;
l - length ;
m - mass of boat;
q - dynamic pressure, $\rho V^2/2$;
Δ - displacement of boat;
ψ_a - yaw angle (aerodynamic), the angle between the midspan chord of the soil and the aerodynamic wind vector $\underset{\sim}{V}a$;
ψ_h - yaw angle (hydrodynamic), the angle between the hull centerline and the boat velocity vector $\underset{\sim}{V}b$;
Ω - angular velocity;
β - boat velocity vector ($\underset{\sim}{V}b$) angle to apparent wind vector ($\underset{\sim}{V}a$)... see Figure 2;
δ_a - "drag angle" (aerodynamic), $\delta_a = \tan^{-1} D_a/S_a$;
γ - $(\beta - \delta_a)$, by definition;
θ - twist angle, defined as the angle between the sail chord and the boom;
ν - kinematic viscosity of the fluid medium;
ρ - density of the fluid medium;
σ - sail angle relative to boat centerline, $\sigma \approx (\gamma - \psi_h)$;
τ - true wind angle relative to boat velocity vector (see Figure 2);

Subscripts:

D - drag;
L - lift;
R - resultant force;
S - sideforce;
a - aerodynamic;
b - boat or board where appropriate;
c - crew;
f - friction;
h - hydrodynamic;
i - induced;

p - parasite;
s - sail;
t - true;
w - water;
* - indicates differentiation with respect to time;
~ - indicates a vector quantity;

INTRODUCTION

The mechanics of sailboat performance involves aerodynamic as well as hydrodynamic considerations. Both sails and hull serve as "lifting" surfaces in the aerodynamic sense. The sail utilizes the reaction with the apparent wind to provide thrust and the hull operates at an angle of yaw to develop the side force which counteracts leeway. The similarity to the operation of aeronautical lifting surfaces is obvious. As a result, one might expect that much aerodynamic data on wings accumulated from decades of experience in aeronautical engineering would combine with hydrodynamic data on hulls to permit the prediction of the performance of a specified sailing yacht.

So far, attempts to apply such information have not met with notable success. One reason is that the aerodynamics of the traditional sailing yacht is quite complicated when compared to that of the average glider or subsonic airplane. The complication is partly due to the aerodynamic interaction among such elements as multiple softsails, exposed standing and running rigging, hulls and crew, and surface waves. The underwater lifting surfaces are also complicated by low aspect ratio and by the necessity for operation at or near the air-water interface. In addition, the motion of a yacht is essentially unsteady motion. The disturbance velocities due to gustiness and wave motion are frequently not small relative to a characteristic velocity of the yacht. Thus, even though steady state analyses are useful for airplane performance predictions, there is some question, in the practical sense, concerning the applicability of such analyses to yacht performance. Another difficulty in the

analysis is due to the coupling which occurs among aerodynamic and hydrodynamic variables. For example, a sudden gust may increase the sail force which increases heel and leeway, decreases thrust, and increases the hydrodynamic drag, and so on. Finally, the scarcity of published results of performance investigations and of aerodynamic investigations of sails and hulls makes it difficult to evaluate simplifying assumptions which would make the problem tractable.

Although the groundwork for systematic performance analysis has been laid (see, for example, Davidson[1] [1956]), a comparison between predicted and measured performance together with an evaluation of the methods does not appear to be generally available.

Tanner [1962] identified the variables in the problem, discussed the coupling among variables, and described graphical solutions of general utility for somewhat restricted operating conditions and for plausible physical restrictions. However, no performance data were given. Herreshoff [1964] discussed the application of the digital computer to the solution of the steady state equations of motion. Taken together with intensive model testing and performance testing of a given yacht, this procedure would be expected to yield a maximum of precise information useful for optimizing a specific design as well as for predicting its performance. However, these facilities and techniques are not generally available.

---

1. References are listed alphabetically by author's name at the end of the paper.

Myers [1964] published a steady state theory for catamaran performance. A special effort was made to account for all major factors influencing sailing performance. A comparison of the predicted performance of individual boats with measured results indicated "that they do not appear to disagree with the theory within the limits of the measurement accuracies." However, as Myers pointed out, the measurements tended to be "an order-of-magnitude less accurate than desired for a careful comparison of theory and experiment." Furthermore, to obtain theoretical results for a specific boat requires the solution of a rather complicated algebraic expression. For the average yachtsman the manual labor required to obtain a solution (sans machine) is formidable. In view of these circumstances it would seem reasonable to sacrifice some theoretical sophistication and/or breadth of application in the hope of gaining simplicity and perspective. A simple algebraic solution would undoubtedly be of greater convenience. Presumably, it would provide approximate performance information over a reasonably wide range of operating conditions and sailing vehicle configurations. One object of the present investigation was to produce such a theory.

To obtain a readily usable solution required some seemingly drastic physical simplification of the theory. In order to gain some idea of the range of validity of the approximations, performance data were required. Thus, the second, equally important objective of this investigation was the development of a straightforward technique of performance testing. As a result of this development, sailing performance data were obtained from a fourteen foot catamaran over a reasonable range of conditions and configurations. The limits of applicability of the theoretical result were then examined in terms of the experimental results.

PART I

THEORY

The motion of a sailing vehicle can be described concisely by two vector equations which provide sufficient generality to cover most operating conditions. These are simply mathematical statements of the principles of conservation of the linear momentum and the angular momentum, respectively, of the vehicle. Thus[1]

$$\underset{\sim}{R}_a + \underset{\sim}{R}_h + (\rho\Delta + m)\underset{\sim}{g} = m\dot{\underset{\sim}{V}}_b + \underset{\sim}{\Omega} \times m\underset{\sim}{V}_b \qquad (1)$$

and

$$\underset{\sim}{C}_a + \underset{\sim}{C}_h = \dot{\underset{\sim}{a}} + \underset{\sim}{\Omega} \times \underset{\sim}{a} \qquad (2)$$

for coordinate axes fixed in the center of gravity of the vehicle. In these equations,

$\underset{\sim}{R}_a$ represents the resultant aerodynamic force vector;

$\underset{\sim}{R}_h$ is the resultant hydrodynamic force vector;

$(\rho\Delta + m)\underset{\sim}{g}$ is the time dependent net force resulting from differences between buoyancy and the weight of the boat;

$m\dot{\underset{\sim}{V}}_b$ is the rate of change of momentum due to linear acceleration;

---

1. Definitions of the symbols used will be found in the table of nomenclature.

$\underset{\sim}{\Omega} \times m\underset{\sim}{V}_b$ is the rate of change of linear momentum due to combined pitching, heeling, and yawing motions.

In equation (2),

$\underset{\sim}{C}_a$ is the couple about the c.g. due to action of the aerodynamic resultant force;

$\underset{\sim}{C}_h$ is the couple due to the hydrodynamic force;

$\dot{\underset{\sim}{a}}$ is the rate of change of angular momentum resulting from net couple action;

$\underset{\sim}{\Omega} \times \underset{\sim}{a}$ is the rate of change of angular momentum due to combined pitching, heeling, and yawing motions.

These equations are quite general in their application[1]. They have not yet been solved in this generality as applied to sailing vehicles nor will a general solution be attempted here. Nevertheless, they are useful in the present context as a framework in which to exhibit the various physical factors entering the problem in its utmost generality. Furthermore, comparison of the drastically simplified version of the equations to be solved below with equations (1) and (2) will keep the approximate nature of the present solution clearly in perspective.

Herreshoff [1964] expressed the cartesian components of the time dependent motion equations (1) and (2) in expanded form. However, no discussion of a possible solution of the complete equations was attempted.

---

1. For details of their development for application to the analysis of the motion of aircraft see, for example, Milne-Thomson[1947].

Tanner [1962] had previously suggested several physical restrictions which simplify the problem. The first of these is the assumption of steady sailing conditions. This is tantamount to the assumption that time averaged quantities characterizing the performance can be defined over a limited period of time. This hypothesis of a "quasi-steady" character of flow fields has been successfully employed for many years in other areas of fluid mechanics and it is upon this justification that the assumption rests. Thereby, equations (1) and (2) reduce immediately to

$$\underset{\sim}{R}_a + \underset{\sim}{R}_h = 0 \qquad (3)$$

and

$$\underset{\sim}{C}_a + \underset{\sim}{C}_h = 0 \qquad (4)$$

A problem in static equilibrium results. The range of validity of a solution based on this restriction may be small in view of the well known unsteadiness of the motion. However, it greatly simplifies the problem and in the absence of contradictory data it will be assumed valid. The range of validity may be determined empirically.

Several other suggestions by Tanner will also be adopted. Disregarded are: i) heel angle; ii) vertical components of the resultant forces $\underset{\sim}{R}_a$ and $\underset{\sim}{R}_h$; iii) pitch (or trim) angle; and, iv) changes in attitude due to changes in pitching and heeling moments. These approximations seem especially appropriate for application to the catamaran. For normal operation, heel

angles are restricted to less than ten degrees. In view of this, assumptions i) and ii) are plausible. The catamaran attitude is comparatively sensitive to changes in pitching moment because of the fine bows. However, for normal operation the pitch angle and heel angle are of the same order of magnitude. furthermore, for daysailing and racing catamarans the crew weight is usually of the same order as the weight of the boat. Thus, changes in heel and pitch can be compensated by shifts in crew position. On these grounds, the pitch angle is assumed negligible and the neglect of changes in attitude with changes in magnitude of pitching and heeling moments is likewise justified. Other vehicles which seem frequently to operate within these restrictions are the trimaran and planing monohulls equipped with trapeze for heel control.

The foregoing restrictions reduce the problem to the consideration of equilibrium in the plane of the water's surface. In view of the neglect of effects of changes in heeling and pitching moments, it is of interest to consider the plausibility of neglecting changes in yawing moment.

Figure 1 is a diagram illustrating the forces remaining in the simplified problem. Body axes are chosen with the origin in the center of gravity of the vehicle. The x-axis lies in the plane of symmetry of the hulls, parallel to the plane of the load waterline, and measured positive forward. The y-axis is perpendicular to the plane of symmetry and positive to starboard. The z-axis is perpendicular to the plane containing the load waterline and is measured positive downward. The components of the aerodynamic and hydrodynamic resultants are shown in the figure.

The remaining components of equations (3) and (4) may be written

$$R_{a_x} + R_{h_x} = 0 \tag{5}$$

$$R_{a_y} + R_{h_y} = 0 \tag{6}$$

$$M_{a_z} + M_{h_z} = 0 \tag{7}$$

The vertical component of the force equation is automatically satisfied for the steady state condition*

If it is assumed that the rudder force is zero, equation (7) is also automatically satisfied.[2] Attaining this condition is like trimming for neutral static stability in an airplane. In the case of a sailboat, it is usually possible to achieve balance over a large portion of the operating range by tuning within the limitations of adjustment of the aerodynamic and hydrodynamic surfaces. Hence, the assumption that equation (7) is automatically satisfied is justified to the degree that neutral static stability ("balance") about the z axis can be maintained over a range of headings to the wind.

In summary, equations (1) and (2) are simplified by the following restrictions:

1) the flow is regarded as steady and the water surface as "flat"[1];

2) vertical components of the aero-and-hydrodynamic resultant forces are neglected;

---

* This implies that only hydrostatic buoyancy is effective; i.e., the hydrodynamic lifting force which leads to planing is ignored.

1. "Flat" is defined by the condition that a characteristic wavelength is small compared to the waterline length of the hull.

2. Implicit is the assumption that R_a and R_h act at the same distance from c.g. (Figs. 1 and 2).

3) the rudder normal force is assumed zero;

4) all moments are neglected;

5) heel and pitch angles are assumed zero;

6) variations in sail shape with dynamic pressure are neglected.

The last assumption is based partly on the common use of fully battened or other "hard" mainsails by catamarans. Variations in the shape of foresails are simply ignored and this assumption remains to be investigated.

It is obviously desirable to express the performance in terms of the boat velocity vector and the wind velocity vector. This is more conveniently done in terms of the aerodynamic and hydrodynamic quantities defined on Figure 2. In this figure, axes are fixed in the boat and velocities are as the helmsman sees them; i.e., the velocity of the water relative to the boat is $\underset{\sim}{V}_h \left(= -\underset{\sim}{V}_b \right)$ and the wind velocity is the apparent (or aerodynamic) wind $\underset{\sim}{V}_a$. Considering components of force parallel and perpendicular to the hydrodynamic velocity yields for equilibrium that

$$R_a \sin(\beta - \delta_a) = D_h \tag{8}$$

and

$$R_a \cos(\beta - \delta_a) = S_h \tag{9}$$

; i.e., thrust equals drag and the aerodynamic resultant force component perpendicular to the hydrodynamic velocity vector equals the hydrodynamic sideforce.

The hydrodynamic drag can be expressed in terms of its elements as

$$D_h = [D_o + D_f + D_w] + D_i \tag{10}$$

and, following Myers [1960], the profile, friction, and wave drags are lumped together with only the hydrodynamic induced drag being considered separately. Next, it is assumed that

$$D_h = k D_f + D_i \tag{11}$$

satisfactorily approximates equation (10) over the operating range anticipated. The plausibility of this assumption is based on towing tank data for high fineness ratio, light displacement hulls (Eggers [1955]; Gluntz [1957]; Havelock [1951]; Henry [1955]; Marchaj [1964, p.242]; Mehaffy [1960]; Wehausen [1956]; Wigley [1949]).* In equation (11), the coefficient

$$k = 1 + \frac{D_o + D_w}{D_f} \tag{12}$$

is evaluated from tank data.

In a later paper dealing with cruising catamarans, Myers [1964] discarded this assumption in favor of a more sophisticated approach. However, the present paper is concerned solely with hulls that have the capability of semi-planing.** With this in mind and in view of the experimental uncertainties of existing performance data, the use of equation (12) is considered justified. Its incorporation into the analysis adds considerably to the ease of practical application of the final result.

After the last term of equation (11) is expressed in terms of the ratio D_i/S_h and force coefficients are defined $\left(C \equiv F/\left(\rho \frac{V^2 A}{2}\right)\right)$ using appropriate areas and velocities, equations (8), (9), and (11) can be

* See also, Savitsky, 1964, Marine Tech., Vol. 1, No. 1, Oct. 1964, p. 71, (eqn. 25).

** Hulls of displacement form (such as cats) where loads are $\ni \frac{\nabla}{(.01L)^3} < 45$

combined to yield

$$\left[\frac{V_b}{V_a}\right]^2 = \frac{\rho_a}{\rho_w}\frac{C_{Ra}}{\lambda C_f}\frac{A_s}{A_s}\left[\sin(\beta-\delta_a)-\left(\frac{C_{Di}}{C_s}\right)_\lambda \cos(\beta-\delta_a)\right] \qquad (13)$$

where $C_{Ra} = \dfrac{2R_a}{\rho_a V_a^2 A_s}$; $C_f = \dfrac{2D_f}{\rho_w V_b^2 A_f}$

$$\delta_a = \tan^{-1}(D_a/S_a)$$

Equation (13) expresses the ratio of boat speed to apparent wind speed as a function of heading to the apparent wind (β) and other measurables of the problem. Of the latter, the air and water densities are thermophysical properties and can be obtained from tabulated values when the temperature and pressure are known. The air density can easily vary as much as 10% under normally encountered operating conditions. Therefore, this ratio should not arbitrarily be assumed invariant.

The sail area (As) can be taken as a parameter if it is assumed that the "effective" sail area is equal to the geometric sail area of a given configuration. Accordingly, it will be assumed hereafter that As is the total geometric sail area in use.

For lightweight planing hulls, the friction (or wetted) area (A_f) depends on hull shape, boat weight, crew weight, board and rudder design, and dynamic lift. The latter has been assumed negligible for the present purpose. With this restriction, A_f becomes a parameter. It can be determined in an individual case from the lines and knowledge of the boat weight, crew weight, and board and rudder areas at a given heading. An example of an empirical equation for A_f for the DC14-P is given in Appendix A.

As previously mentioned, the coefficient λ must be determined from towing data at zero yaw. Naturally, equation (11) is only an approximation

and the accuracy of the result will vary for individual hull forms. However, given towing tank data, the error in $[V_b/V_a]$ due to the approximation can be determined. For example, in the case of the International Canoe (Marchaj [1964], p. 242), equation (11) over-estimates the zero yaw drag between zero and five and a half knots hull speed. Between five and a half and 10 knots, the drag is underestimated by equation (11). The maximum error is approximately 25%. The mean error in drag is roughly 10%. However, in view of the primitive present state of the art with respect to understanding sail aerodynamics and in predicting hull induced drag characteristics, equation (11) will be accepted because of the generality that this assumption brings to the analysis.

The skin friction coefficient (C_f) for smooth surfaces depends on the boat velocity V_b (through the Reynolds number $V_b l/\nu_w$) as is well known (see, for example, Marchaj [1964], Part III, §1; or Schlicting [1955]). However, for "rough" surfaces, the friction coefficient is approximately constant over most of the operating range of the configurations considered here (Schlicting [1955], p. 448).[1] Specifically, it will be assumed that

$$C_f = \left[1.89 + 1.62 \log_{10}(l/k_s)\right]^{-2.5} \qquad (14)$$

where $l \sim$ waterline length;
$k_s \sim$ surface roughness.

Typical values of practical surface roughnesses are found in Hoerner [1965],

---

1. For convenience, a plot of C_f versus R_l for parameters of roughness is shown in Appendix A as Figure A-2.

p. 5-3. For boats of 12 feet and up and for a surface roughness equivalent to or greater than that of smooth marine paint, equation (14) is applicable for boat speeds greater than about two knots. Details of a calculation of this quantity for a fourteen foot catamaran are given in Appendix A.

From the foregoing discussion it appears reasonable to regard ρ_a/ρ_w, A_s, A_f, k, ε, C_f as parameters of the performance equation within the framework of physical restrictions specified. It remains to supply auxilliary equations for $[C_{D_i}/C_s]_\lambda$, δ_a and C_{R_a}.

The ratio of hydrodynamic induced drag to hydrodynamic sideforce (Figure 2) depends mainly on the magnitude of the hydrodynamic sideforce (equation (9)) and the geometry of the hull below the waterline (see, for example, Marchaj [1964], p. 270). Letcher [1965] suggested the application of the lifting line theory from aeronautics to the evaluation of $[D_i/S]_\lambda$ in terms of the hydrodynamic sideforce and hull geometric and hydrodynamic parameters. Applying this theory to the present case and expressing the hydrodynamic sideforce in terms of the aerodynamic resultant force through equation (9) yields

$$\left[\frac{C_{D_i}}{C_s}\right]_\lambda = \frac{1}{\pi}\frac{\rho_a}{\rho_w}\frac{A_s}{A_i}\frac{C_{R_a}\cos(\beta-\delta_a)}{e_b R}\left[\frac{V_a}{V_b}\right]^2 \qquad (15)$$

where A_i - projected hull and board area effective in producing sideforce;

R - effective draft to chord ratio of the hydrodynamic surface which produces sideforce;

e_b - efficiency factor.

More detailed discussion is provided in Appendix A.

Clearly, the hydrodynamic induced drag to sideforce ratio varies considerably with heading to the apparent wind and with the relative boat speed. Furthermore, the induced drag may vary from zero to a magnitude several times that of the unyawed hull drag over the normal operating range. Finally, there is an additional implicit dependence of $[C_{D_i}/C_s]_h$ on β through the functions $C_{R_a}(\beta)$ and $\delta_a(\beta)$ which remain to be considered. Hence, there is no obvious justification for assuming parametric values for the hull induced drag to sideforce ratio. The ratio $[C_{D_i}/C_s]_h$ must be regarded as a dependent variable of the problem. The remaining variables are the aerodynamic drag to sideforce ratio (δ_a) and the aerodynamic resultant force coefficient (C_{R_a}). Although these quantities are known to vary with β (at least), no general theory exists at present for predicting this dependence for a given configuration.

The strong similarity between sails and the lifting surfaces employed in aeronautical engineering is commonly recognized. However, the average sailboat rig is very complicated, aerodynamically speaking, by the presence of multiple soft sails of odd shapes, variable gaps, standing and running rigging, crew, and hull(s). Furthermore, present day rigs are operated in a partially or completely stalled condition most of the time. As a result, the average aerodynamicist is appalled at the prospect of having to attempt a prediction of the aerodynamic resultant force vector for all possible headings to the apparent wind. If it were possible to do so, both $C_{R_a}(\beta)$ and $\delta_a(\beta)$ would be determined and the prediction of performance within the present physical restrictions would be accomplished. However, such is not the case. Although attempts at

a semi-empirical theory are being made, progress in this direction is slow.

Early attempts at a two dimensional theory for inviscid flow (Thwaites [1961]) have been followed by the application of finite wing theory to (unstalled) "soft" sail wings of finite aspect ratio. (Nielsen et al [1963]). The application of the finite wing theory was to paragliders a comparatively clean aerodynamic configuration compared to the average sailboat. Thus, the direct use of these results even in the unstalled regime of sail operation is probably not justified in the absence of experimental results, such as wind tunnel tests on sailboat configurations. A comparison of Nielson's predictions with existing sail test data has not yet been attempted to the present author's knowledge.

Prior to 1960, most of the available sail data consisted of wind tunnel tests at very small scale on sheet metal wings. Since that time, a certain amount of sail data has been published in the open literature. Marchaj [1964] summarized much of the existing data on metal models of single sails. In addition, he included in his book data obtained from wind tunnel tests on larger scale cloth sails at the University of Southampton. Results of 1/4 scale tests of hull, mainsail, and genoa in combination carried out by Marchaj and Tanner were reported in the open literature by Richards [1965]. These data were limited to the close hauled condition. Full scale aerodynamics tests of an International 12 dinghy have been reported by Bruce [1962]. The data were obtained from measurements in the full scale boat tethered to a mooring with a suitable force measuring device. There is an obvious advantage in testing at full scale in the natural wind so far as "modelling" is concerned. Inclusion of studies of effects of hull, helmsman and crew, and rigging is no great problem. Finally, such tests permit the investigation to range over

all possible values of heading to the relative wind (β). However, the inherent experimental uncertainty is much greater than for wind tunnel tests at present.

Although the empirical results just described are necessarily limited in scope, they can be used to establish some realistic bounds on the functions $C_{R_a}(\beta)$ and $\delta_a(\beta)$. With this much help, sufficiently realistic sample functions can be postulated to permit establishing some estimates of physical limits on performance. This will be attempted in the following paragraphs.

Combining equations (13 and (15) yields

$$\left[\frac{V_b}{V_a}\right] = \left[\frac{a C_{R_a}(\beta)}{2}\left[\sin(\beta-\delta_a) + \sqrt{\sin^2(\beta-\delta_a) - \frac{4b}{\pi}\cos^2(\beta-\delta_a)}\right]\right]^{1/2} \qquad (16)$$

where

$\frac{a C_{R_a}(\beta)}{2} = \frac{1}{2}\left[\frac{\rho_a A_s C_{R_a}}{k_2 \rho_w A_f C_f}\right]$ represents the ratio of available aerodynamic force to the zero yaw hull drag, (for brevity this will be referred to as the "thrust index" in what follows;

$\frac{4b}{\pi} = \frac{1}{\pi}\left[\frac{k C_f A_f}{e_b AR A_i}\right]$ represents the product of the zero yaw hull drag and the hull induced drag; (this will, hereafter, be termed "hydrodynamic drag product";

and

$\left(\beta - \delta_a(\beta)\right) \equiv \gamma$ is the difference between the heading to the apparent wind and the aerodynamic drag angle; note that $(90-\gamma)$ is the angle between $\underline{C}_{R_a}$ and $\underline{V}_a$.

In equation (16) a choice of the negative root implies that decreasing the drag results in a decrease of apparent boat speed ratio which is physically unrealistic. Therefore, the positive root was selected.

A limit on the solution is imposed by the fact that the quantity under the radical is negative for a certain range of $(\beta - \delta_a)$ regardless of the magnitude of $b > 0$. Physically speaking, the appearance of the imaginary root implies that the fundamental hypothesis is no longer applicable; i.e., static equilibrium is no longer possible. Intuitively, this situation corresponds to pinching to the point where the boat speed is no longer great enough to develop the sideforce required to balance the leeway component of the aerodynamic resultant force and the boat "falls off"; i.e., acceleration occurs. This condition can be expressed in terms of the ratio of aerodynamic thrust to hydrodynamic sideforce; viz; when

$$\frac{T}{S_L} < \frac{4k\, C_f A_f \cot(\beta - \delta_a)}{\pi e_0 AR A_i} \qquad (17)$$

static equilibrium in the balanced condition (which was postulated) can no longer be maintained. Thus, a "pointing" limit is represented by equation (17). To improve pointing, equation (17) indicates that it is necessary to minimize the aerodynamic drag to lift ratio as well as the zero yaw hull drag and the hydrodynamic induced drag. Although not a revolutionary idea, this is in qualitative agreement with practical experience and lends credence to the theory.

In order to obtain a complete picture of the performance, it is necessary to transform equation (16) to earth fixed axes. This can easily be done by referring to Figure 2. According to the velocity triangle, the

heading with respect to the true wind can be written as

$$\tau = \tan^{-1}\left[\frac{\sin\beta}{\cos\beta - (V_b/V_a)}\right] \tag{18}$$

which is the expression of the heading with respect to the true wind in terms of the apparent wind direction and the apparent boat speed ratio. Similar considerations yield (since $|\underline{V}_b| = |\underline{V}_a|$)

$$\frac{V_b}{V_t} = \frac{1}{\sqrt{\left(V_a/V_b\right)^2 + \cos^2\tau - 1} - \cos\tau} \tag{19}$$

the true boat speed ratio in terms of the apparent boat speed ratio and the heading to the true wind direction.

Predicted Performance for the Cantilevered Unirig. With the help of postulated functions $C_{R_a}(\beta)$ and $\delta_a(\beta)$, equations (16), (18), and (19) provide the desired performance prediction. For the present investigation two such functions were formulated based on possible but simplified operating configurations. The first assumed a balanced cantilevered unirig with circular mainsheet tracks. With this arrangement, a constant angle of the sail to the apparent wind as well as constant sail shape could be maintained for all headings. Therefore, C_{R_a} and δ_a are independent of β. The second case was chosen to approximate the stay limited operation of conventional rigs.

Sketches of the first configuration are shown on Figure 3. The aerodynamically balanced sail pivots about its chordwise center of pressure. Thus, when trim for neutral helm is established on one heading it is maintained on all headings assuming negligible hydrodynamic center of pressure travel with

hull yaw. Constant aerodynamic yaw angle (ψ_a) is maintained regardless of heading. Therefore, C_{R_a} and δ_a are constant.

An obvious inference from equation (16) is that for maximum performance on all headings a given configuration should be operated at maximum aerodynamic resultant force ($C_{R_{a\,max}}$) and at minimum aerodynamic drag angle ($\delta_{a,min}$). However, it will be shown in what follows that this is not always the case. In any event, since for practical configurations these two values do not occur at the same aerodynamic yaw angle, a compromise is necessary. For the present example, average values were chosen from the aerodynamic data previously referenced. Specifically, ranges $\left(1.0 \leq C_{R_a}]_{max} \leq 1.8\right)$ and $\left(5^\circ \leq \delta_a]_{min} \leq 20^\circ\right)$ are possible. In the latter case, the 5° limit represents the aerodynamic drag angle for a complete airplane of vintage 1940 (Wood [1955], p. 14-20). The 20° upper limit is approximately that measured by Bruce [1962] in his tether testing of the International 12 Dinghy.

It was desired to compare the predicted performance of a boat of the configuration just postulated (Figure 3) with the measured performance of the boat of the present investigation. Therefore, the geometric characteristics of the measured boat were used in determining a range of values for parameters "a" and "b" of equation (16). The boat data are found in Table I and also in Appendix A where more detail is provided. It was necessary to provide a range for C_f (depending on wetted surface roughness) and for e_b, the hydrofoil efficiency factor. A reasonable range for C_f based on equation (14) was specified as $0.0025 < C_f < 0.0050$. In the absence of hydrodynamic data, a rough estimate of e_b was obtained from aerodynamic data (Wood [1955], p. 9-15). The range selected was $0.35 < e_b < 0.75$.

These approximations together with the geometry of the experimental boat gave the following ranges: for thrust index, $.19 < \frac{a C_{R_a}}{2} < .58$; for hydrodynamic drag product, $.03 < \frac{4b}{\pi} < .13$; and for aerodynamic drag angle, $5 < \delta_a < 20$.

Values of the performance parameters outside this range may be obtained in practice by variation of the sail area to wetted area ratio (A_s/A_f) ; the ratio of wetted area to effective hydrodynamic sideforce producing area $(A_f/e_b A_i)$; the ratio of zero yaw hull drag to friction drag (k); and the hydrodynamic aspect ratio ($\mathcal{R}$). A maximum possible value for the thrust index based on "best guesses" for these values was chosen as $\left.\frac{a C_{R_a}}{2}\right]_{max} = 1.5$. Similarly, limiting values of the hydrodynamic product were chosen as 0.02 and 0.20. The aerodynamic drag angle range of the preceding paragraph would appear to cover a sufficiently wide range of configurations.

Performance calculations based on these ranges of the three performance parameters are shown as Figures 4 through 8. Physically, these curves represent the possible variations in performance of the configuration of Figure 3 by changing performance parameters. The results hold for all boats of the general configuration of Figure 3 regardless of size as long as they operate within the physical restrictions placed on the theory. The most important of these conditions in probable order of difficulty of attainment over a wide range are: a parabolic hydrodynamic drag curve; balance on all headings; and approximately zero heel. Further conjecture about the limits of applicability of the theory is useless in the absence of experimental results. However, a detailed discussion of the physical significance of the plotted results is in order.

Figure 4 is a plot of equation (16) over the range of performance parameters specified above. Shown is the apparent boat speed ratio $[V_b/V_a]$ versus τ . Note that $(90-\tau)$ is the angle between the aerodynamic resultant force coefficient vector C_{R_a} and the boat velocity vector V_b (see Figure 2). Thus, when $\tau = 90$, the aerodynamic resultant force is parallel to the boat velocity vector; the hydrodynamic induced drag is zero; and (V_b/V_a) is a maximum for all values of performance parameters. This condition is shown schematically as Figure 3c). As $\tau \to 0$, the aerodynamic resultant becomes nearly perpendicular to V_b , the hydrodynamic induced drag effect becomes maximum and the pinching limit previously discussed is reached. This condition is shown as Figure 3a). As $\tau \to 180$, for a boat of this configuration the induced drag again becomes large and a downwind pinching limit is reached. That this should be true is obvious from Figure 3e).

It is reasonable on the basis of experience that parasite aerodynamic drag should be minimized going to windward and maximized running downwind. Note that if the results of Figure 4 are expressed as $[V_b/V_a]$ versus β , increasing the aerodynamic drag angle δ_a is harmful to performance upwind but beneficial to downwind performance for this configuration as would be expected. Experience would indicate that the best procedure for best all around performance would be to minimize δ_a except when broad reaching or running when the sail should be stalled (thereby increasing δ_a) for best performance. It will be shown later that this procedure is not necessarily valid with the configuration of Figure 3.

Figure 4 shows that the maximum apparent boat speed ratio $[V_b/V_a]$ depends solely on the thrust index; i.e., it is independent of the hydrodynamic drag product as well as the aerodynamic drag angle. However, such is not the

case so far as the true boat speed ratio is concerned.

This can be seen on Figure 5 where the true boat speed ratio V_b/V_t versus the angle τ between the boat velocity and the true wind vectors is plotted. Only one value of aerodynamic drag angle $\varepsilon_a = 15°$ is shown. From this presentation it is clear that the maximum true boat speed ratio does depend on the hydrodynamic induced drag. Calculations show that it also depends on the aerodynamic drag angle as would be expected. The sensitivity to aero-and-hydrodynamic cleanliness is greater the greater the maximum speed of the boat. Thus a very "powerful" boat $\left(\frac{a C_{Ra}}{2} = 1.5, \text{say}\right)$ with a very "dirty" hull $\left(\frac{4b}{\pi} = 0.2\right)$ and a fairly "dirty" rig $(\varepsilon_a = 15°)$ reaches her pinching limit at $98°$. Whereas, if the induced drag of the hull could be sufficiently reduced $\left(\frac{4b}{\pi} = 0.02\right)$, the pinching limit wouldnot be encountered until $\tau = 58°$, a 40 degree improvement. The attendant improvement in true boat speed ratio is roughly 20%. For the least "powerful" boat $\left(\frac{a C_{Ra}}{2} = 0.2\right)$, the pinching limit is decreased by only 24 degrees and the maximum boat speed ratio by just 3.3%.

Note that the pinching limit does not imply the limit of progress of a given boat to windward. It simply means that in order to maintain steady progress along a more weatherly course, the aerodynamic leeway force component must be reduced. This may be done by reducing ψ_a (thereby, C_{Ra} & $\frac{a C_{Ra}}{2}$). On Figure 5, such a "pinching line" is shown for the case where $\frac{4b}{\pi} = 0.0675$ and $\varepsilon_a = 15°$. By following the pinching line from $\left(V_b/V_t\right) = 1.3$ to 0.3, it can be seen that the more powerful boat of given cleanliness will sail just as close to the true wind as the less powerful equally clean boat. However, it is necessary to reduce C_{Ra} in order to do so. Of course, operable

alternatives in the small boat are reducing $\frac{4b}{\pi}$ by increasing A_i or reducing ε_a by "streamlining" the crew at $C_{R_a}]_{max}$; i.e., there are several ways to move along a locus of pinching lines. However, the present calculations assume that the hydrodynamic drag product and the aerodynamic drag angle are held constant as the pinching limit is approached. Pinching is then accomplished by reducing C_{R_a} as described above.

Figure 5 shows the broad reaching and running performance of the Figure 3 configuration to be relatively poor. That this is reasonable can be seen by reference to Figure 3d), e). In broad reaching, the configuration develops an aerodynamic force component to windward. In addition to producing a heeling moment to windward, this windward aerodynamic component must be resisted hydrodynamically, and induced drag results. Also, the thrust component of the aerodynamic resultant is reduced because of its windward angle and, finally, the apparent wind speed is small relative to the true wind speed in this quarter.

This last mentioned effect is shown on Figure 6 where the ratio V_a/V_t is shown versus the true wind angle τ . For clarity, only two values of thrust index and one value of hydrodynamic drag product and aerodynamic drag angle are shown. Shown, also, are corresponding plots of apparent wind angle β versus true wind angle τ . The general characteristics of the curves for $0 < \tau < 130$ are in accord with experience. From the pinching limit, the apparent wind increases to a maximum as the boat heads off. The maximum apparent wind is attained close reaching. As the true wind comes abeam, the apparent wind speed decreases continuously. The variation is greater with the faster boat. The apparent wind speed equals true wind speed at roughly $\tau = 110^\circ$. The "hook" in $\left[V_a/V_t\right]$ for $130 < \tau < 180$ is explained in terms of Figure 3d), e). It comes as a result of the disadvantages previously discussed of attempting to

operate with the aerodynamic resultant force pointing out to windward as shown in the diagrams of Figure 3. As the true wind angle τ, ranges from about 150° to 180° the performance with this configuration simply falls off so rapidly that a net gain in apparent wind speed results. Figure 7 shows that this is a region of operation to be avoided with this configuration even with a slow boat.

Figure 7 is the polar representation of the results plotted in Figure 5. The direction of the true wind and the sense of the boat velocity vector are shown on the diagram. The component of $[V_b/V_t]$ parallel to the true wind direction is the speed made good to windward or downwind depending on the sense of the projection. Thus, continuing the discussion of the previous paragraph, for $150 < \tau < 180$ the best speed downwind will be made by bearing up and tacking downwind with this configuration for even the slowest boat. The course angles for best speed downwind range from 145° for the slowest boat to 132° for the fastest boat.

For tacking to windward with the two slower boats, it can be seen from Figure 7 that the best speed to windward is attained at headings prior to onset of the pinching limit. However, with a very fast boat the indication is that the maximum windward performance would be obtained in the pinched condition; that is, with an aerodynamic resultant force coefficient less than that actually attainable with the rig.

Possible effects on performance of variations of thrust index and drag product were illustrated on Figures 5 through 7. However, the aerodynamic drag angle was held constant at $\delta_a = \tan^{-1}[D_a/S_a] = 15$ degrees. On Figure 8, the effect of varying δ_a between 5 and 20 degrees is shown for the intermediate values of thrust index and drag product. Since

small δ_a is associated with aerodynamic "cleanliness", it is clear that the cleaner boat is faster on all headings (when tacked downwind).

The present calculations indicate the possibility of approaching a maximum true boat speed ratio of 1.2 with an exceptionally fast boat of the configuration of Figure 3. "Fast" in this context implies limiting values of thrust index, drag product, and aerodynamic drag angle which are "best guesses" based on the limited data available. The results shown on Figure 7 and Figure 8 indicate that for all boats the true wind direction for maximum boat speed moves aft for "dirtier" and for faster boats. For a boat of this sail configuration having the geometric and hull characteristics given in Table I performance would be expected to fall on a polar somewhere between the $C_{R_a} = 0.46$ and $C_{R_a} = 0.20$ curves on Figure 7.

Predicted Performance of the Stay Limited Unirig. A sail configuration frequently encountered among current racing catamarans of all sizes is the "stay limited" unirig configuration previously mentioned. The configuration sketched on Figure 9 was assumed for comparison with the previous example as well as with the boat of Table I. Figure 9a) illustrates the assumed geometry. For $\beta < 50°$ it is assumed that the sail is vang controlled. Thus, with a pivoting mast, the sail shape is unchanged with rotation and the optimum aerodynamic yaw angle ψ_a may be maintained. In other words, for the first 50 degrees of apparent wind range, the sail performance is identical to that of Figure 3a) and 3b). For $50 < \beta < 75$ (between the vang limit and stay limit) the shape is assumed to change although $\delta_a \approx \psi_a \approx 15°$* is assumed maintained by sheeting. As the sail shape changes beyond the vang limit, C_{R_a} is assumed to decrease linearly to a value $C_{R_a}\big]_{180} = 1.2$ which was taken from available measurements. Thus, for $50 < \beta < 180$,

$$C_{R_a} = 1.8 - .0046(\beta - 50) \qquad (20)$$

* This results from assuming R_a sail chord (see Figs 3 and 10 for example).

as shown in Figure 9b). Also, for $\beta > 75$ degrees, it is assumed that

$$\psi_a = \beta - [\text{stay limiting angle}] \tag{21}$$

where the stay limiting angle was assumed to be 60 degrees in this example. If C_{R_a} is assumed perpendicular to the mean sail chord,

$$\psi_a = \delta_a \tag{22}$$

and for the assumed configuration equation (21) can be written

$$(\beta - \delta_a) = 60 \tag{23}$$

for $75 < \beta \leq 180$. This information is given on Figure 9b). A diagram of the operation of this rig for comparison with Figure 3 is shown as Figure 10.

With $C_{R_a}(\beta)$ and $\delta_a(\beta)$ known, the performance for the configuration of Figure 10 was evaluated from equations (16, (18), and (19). The plotted results are given as Figures 11 through 14 for comparison with Figures 4 through 7.

The performance for both rigs is obviously identical for $0 < \beta < 50$. This can be seen by comparing Figures 4 and 11 (bearing in mind that $\beta = \gamma + 15$ for the comparison). For $50 < \beta < 75$, the apparent boat speed ratio falls off slightly due to the decrease in C_{R_a} over this interval. Therefore, the performance for $0 < \beta < 75$ is affected very little.

Figure 12 shows that this range of apparent wind angle covers the closehauled, close reaching, and beam reaching conditions for all values of

the three performance parameters. To emphasize this point, values of $\zeta = 50°$ and $\zeta = 75°$ are shown on Figure 13. It is obvious by comparing Figures 5 and 13 that there is little difference between the performance of the configuration of Figure 3 and that of Figures 9 and 10 through the beam reach.

The comparative performance broad reaching and running is the comparison between the dashed and solid lines on Figure 13. The dashed lines are the results of Figure 5. Except for $163 < \tau \leq 180$, the cantilevered unirig is superior according to this comparison. Furthermore, the polar comparison on Figure 14 shows that by bearing up and tacking downwind with the cantilevered unirig superior performance is obtained even for $163 < \tau \leq 180$. Thus, aerodynamic superiority is indicated for the most efficient rig (cantilevered unirig) on all points of sailing. However, it should be recognized that overall superiority of a practical rig will depend on attaining this aerodynamic efficiency together with a minimum weight to strength ratio and maximum simplicity of operation.

Summary and Conclusions

The present simple theory for the prediction of sailboat performance in calm waters depends mainly on the validity of the following assumed approximations to reality: 1) that a quasi-steady fluid flow exists; 2) that the zero yaw hull drag curve is parabolic in form; 3) that the zero helm and zero heel conditions exist on every heading; 4) that the friction drag coefficient is independent of Reynolds number; 5) that the hull induced drag can be predicted by lifting line theory; and, 6) that the aerodynamic resultant force coefficient and the aerodynamic drag angle depend only on the heading to the relative

wind. Within these restrictions $\left[V_b/V_t\right]$ is independent of the true wind speed V_t.

Three parameters serve to describe the performance potential of boats fitting within the framework of the approximations listed above. These parameters are: a "thrust index" $\left[\frac{\rho_a C_{Ra} A_s}{\rho_w C_f k A_f}\right]$; a "hydrodynamic drag product", $\left[\frac{k C_f A_f}{e_b R A_i}\right]$; and the aerodynamic drag angle, $[\delta_a]$. Of these quantities, C_{Ra} and δ_a may exhibit at least piecewise dependence upon β and may be regarded as psuedoparameters. The remaining quantities depend (within the restrictions stated) solely on the geometry and construction of hull and rig and so are true parameters. Given the necessary parametric values, the performance for any boat may be calculated on every heading to the true wind as is shown by Figures 7 and 14.

For design purposes the theory is useful in predicting comparative performance of different configurations of the same boat. This application was illustrated in detail (Figures 3 through 13) in the preceding sections. As a result of the comparison, it was concluded that a cantilevered, balanced unirig was superior to a stay limited, balanced unirig on all headings if the cantilevered rig was tacked downwind.

The stated limitations of the theory point up the necessity for obtaining experimental information in several areas in order to determine the limits of application of the theory. First of all, it must be experimentally determined whether $\left[V_b/V_t\right]$ is in reality independent of V_t. Secondly, the functions $C_{Ra}(\beta)$ and $\delta_a(\beta)$ must be measured over a broader range of conditions and configurations than has been covered at the present writing. Values of e_b and k must be collected from existing literature and made generally available. Finally, the same service should be rendered with respect to the expression of wetted area A_f in terms of the total sailing weight of the hull types discussed here.

REFERENCES

Bradfield, W.S., (1968). Predicted and Measured Performance of a 14 ft. Catamarn, State University of New York at Stony Brook, Department of Mechanics, Ref. No. _____

Bruce, E. (1962). The Physics of Sailing Craft as Revealed by Measurements at Full Scale. AYRS publication no. 40, 23-52.

Davidson, K.S.M. (1956). Surveys in Mechanics, pp. 431-474, Cambridge University Press.

Eggers, K. (1955). Concerning Drag Relations on Two Hulled Ships, Jahrbuch der Schiffbautechnischen Gesellschaft, 49, pp. 516-539.

Gluntz, D.M. (1957). Sailing Catamarans - Design Considerations and Conculsions from Model Tests. Chesapeake Section SNAME.

Havelock, T.H. (1951). Wave Resistance Theory and its Application to Ship Problems. SNAME Transactions 59, p. 18.

Henry, C., Robillard, G., and Villaflor, J. (1955). Effects of Wave Interference of Catamaran Hulls. Department of Naval Architecture and Marine Engineering. Report No. 173. Massachusetts Institute of Technology.

Hrreshoff, H.C. (1964). Hydrodynamics and Aerodynamics of the Sailing Yacht. SNAME Annual Meeting, paper no. 9.

Hoerner, S.F. (1965). Fluid-Dynamic Drag. Published by the Author.

Letcher, J.S., Jr. (1965). Balance of Helm and Static Directional Stability of Yachts Sailing Close-Hauled. J. Roy. Aero Soc., 69, pp. 242-248.

Marchaj, C.A. (1964). Sailing Theory and Practice. Dodd, Mead and Co., New York.

Mehaffery, W.R. (1960). The Recirculation Tank. AYRS publication no. 32, p. 23.

Myers, H.A. (1960). Fast Sailing Catamarans. Published by the author.

Myers, H.A. (1964). Theory of Sailing - With Application to Modern Catamarans. Marine Technology, October, pp. 10-28.

Milne-Thomson, L.M. (1947). Theoretical Aerodynamics. D. Van Nostrand Co., Inc.

Nielsen, J.N. (1963). Theory of Flexible Aerodynamic Surfaces. J. Appl. Mech., Vol. 30, pp. 435-442.

Prandtl, L. and Tietjens, O.G. (1934). Applied Hydro-and-Aeromechanics. Dover Publications, Inc., New York.

Richards, E.J. (1965). Aeronautical Research at the University of Southhampton. J. Roy. Aero. Soc., Vol. 69, pp. 505-541.

Schlicting, H. (1955). Boundary Layer Theory. McGraw-Hill Book Co., Inc., New York.

Tanner, T. (1962). A Survey of Yacht Research at Southampton University. J. Roy. Aero. Soc., Vol. 66, pp. 642-648.

Thwaites, B. (1961). The Aerodynamic Theory of Sails. Proc. Roy. Soc. A., Vol. 261.

Wehausen, J. V. (1956). Wave Resistance of Thin Ships. Symposium on Naval Hydrodynamics, public. 515, N.A.C., N.R.C., pp. 109-137.

Wigley, W. C. S. and Lunde, G. K. (1949). Transactions INA, Vol. 90, p. 48.

Wood, K. D. (1955). Technical Aerodynamics. Third Edition. Published by author, Boulder, Colo.

APPENDIX A

Evaluation of Performance Parameters

(Adapted from Bradfield [1968])

In order to predict the performance of the boat of the present investigation, it was obviously necessary to assign numbers to the parameters A_s, A_f, k, C_f, C_{Ra}, S_a, and D_j/S_h of equation (13). For convenience, we may rewrite the performance equations

$$\frac{V_b}{V_a} = \left[\left(\frac{\rho_a}{\rho_w}\right)\left(\frac{C_{Ra}}{k C_f}\right)\frac{A_s}{A_f}\left[\sin(\beta-\delta_a) - \frac{D_j}{S_h}\cos(\beta-\delta_a)\right]\right]^{1/2} \tag{13}$$

and

$$\frac{V_b}{V_t} = \frac{1}{\sqrt{\left(V_a/V_b\right)^2 + \cos^2\tau - 1} - \cos\tau} \tag{19}$$

where symbols are defined in the table of nomenclature.

The Density Ratio and Geometric Parameters. The density ratio = $^1/_{835}$ for seawater. The sail area and the wetted area are geometric parameters taken from the design data of the DC-14P class boat. Table I contains data on the boat used in the present investigation. The area of the main is 100 ft^2. The area of the jib is 40 ft^2. The area of the spinnaker is 115 ft^2.

Wetted Area as a Function of Loading. A curve of wetted area versus displacement is shown as Figure A-1. The areas were obtained by numerical integration of the lines. The boat weighed 431 pounds rigged for sailing with racing equipment and without crew. Crew weight parametric lines are shown on the curve. The racing crew is two.

The integration was performed for two conditions of trim. The first was for trim parallel to the design water line. The present boat was over her lines due to excess weight. Therefore, the second condition investigated was for trim by the bows so as to maintain the design waterline at the sterns. The boat was normally sailed in this attitude to minimize profile drag due to separation at the sterns. The difference in hull wetted area is +5 3/4% trimmed by the head. Note that the difference between 200 and 400 pounds of crew weight is + 20%. The total wetted area of the boards was 4½ ft^2. The rudder wetted area was 4 ft^2.

From these data the total wetted area may be expressed in terms of boat weight and crew weight. Specifically, from Figure A-1, and including the projected area of boards and rudders, the empirical equation

$$A_f = .052 W_b + .040 W_c + 2A_b + 2A_{rud} + 10 \qquad (A\text{-}1)$$

is useful to describe the variation of A_f over the practical range of displacements. For the configurations tested,

$$A_f = 40.5 + .04 W_c \qquad (A\text{-}2)$$

A value of k = 2 was chosen for the present boat. This factor was obtained from the published data in full scale towing basin tests of the International Canoe (Tanner [1960]) the geometric characteristics of which are similar to those of the present hulls. No attempt was made to account for mutual interference of the hulls.

The Friction Factor. The skin friction coefficient C_f is presumed to vary with the boat speed Vb through its dependence on Reynolds number defined by

$$R_\ell = V_b \ell / \nu \qquad \text{(A-3)}$$

where ℓ is taken as the sailing waterline length for computing the hull skin friction. For boards and rudders, the hydrodynamic chord is taken as the characteristic length. Assuming that the friction drag of boards and rudders is not negligible and since the ratio of characteristic lengths is of the order (20/1), the different surfaces may operate in different friction drag regions. Therefore, C_f is a weighted mean coefficient defined by

$$C_f = \frac{1}{A_f}\left[A_{hull} C_{f\,hull} + A_b C_{f\,b} + A_{rud} C_{f\,rud}\right] \qquad \text{(A-4)}$$

when individual friction coefficients are determined according to Reynolds number.

A random sample of 35 runs of the present experimental investigation (out of a one hundred eighty-six run total) indicates an arithmetic mean value of boat speed $\overline{V}_b \approx 6.5$ mph. The minimum value recorded was 2.7 mph and the maximum value was 13.5 mph. The corresponding hydrodynamic Reynolds number per foot for this range is roughly $3.2 \times 10^5 < (R_e/\ell) < 1.6 \times 10^6$. If it is assumed that the sailing waterline length is approximately the same as the design waterline length (12.5 feet), the corresponding hull Reynolds number range is $4.0 \times 10^6 <$ Rdwl $< 20 \times 10^6$. The mean value of hull Reynolds number is

$$\overline{R}_{dwl} = 9.75 \times 10^6 \qquad \text{(A-5)}$$

The corresponding value for boards is

$$\overline{R}_{bds} = 0.57 \times 10^6 \qquad \text{(A-6)}$$

based on a mean chord of 0.79 feet. The rudders are represented by

$$\bar{R}_{rud} = 0.48 \times 10^6 \qquad \text{(A-7)}$$

based on a mean chord of 0.66 feet. The hull roughness is judged approximately that of smooth marine paint (Marchaj [1964], p. 241). Therefore, the roughness is 2 mils and $(L/k) = 7.5 \times 10^4$. The variation of C_f with R_e for parameters of roughness is shown for convenience as Figure A-2. Accordingly, $C_{f\ hull} = 0.0033$; $C_{f\ bd} = C_{f\ rud} = 0.0018$. With a 300 pound crew, $A_f = 52.5\ ft^2$ from equation (A-2). Thus, from equation (A-4),

$$C_f = \frac{1}{52.5}\left[44 \times .0033 + 8.5 \times .0018\right] = 0.0031 \qquad \text{(A-8)}$$

Furthermore, examination of the data (and comparison with Figure A-2) show that with hull roughness ratios of $(L/k) < 10^5$, the hull skin friction coefficient is essentially independent of Reynolds number (; ie, of boat speed) for speeds greater than about six miles per hour. Therefore, the assumption of constant C_f appears valid over a reasonable portion of the speed range.

The Hydrodynamic Induced Drag Ratio. In evaluating the hydrodynamic induced drag to hydrodynamic sideforce ratio, Letcher [1965] suggested the application of lifting line theory to the boat underbody which was reflected into the water surface to satisfy the boundary condition in that plane. It was assumed that the water surface is approximately flat. Such a construction of the present boat is shown as Figure A-3. The effective aspect ratio of the boards so reflected is $AR_b = 5.0$ in this case. For the rudders, $AR_r = 4.5$ as reflected. However, in the present case where the rudder is hung from the transom, it performs as a surface piercing hydrofoil and the effective aspect ratio is roughly 2¼.

According to lifting line theory (see, for example, Prandtl and Tietiens [1934] Chapter VI), the drag for hydrofoil surfaces such as the boards shown in Figure A-3 can be expressed

$$C_{D_b} = C_{D_{o_b}} + C_{D_{i_b}} \tag{A-9}$$

where

$C_{D_{o_b}}$ is the profile or "zero lift" drag coefficient of the boards which includes pressure drag and skin friction;

and

$$C_{D_{i_b}} = \frac{C^2_{S_{l_b}}}{\pi A R e_b}$$

is the induced drag or drag due to sideforce of the boards. In the present case, the total drag due to sideforce has been charged to the boards and, hence

$$\frac{C_{D_i}}{C_{S_l}} = \frac{C_{S_l}}{\pi A R e_b} \tag{A-10}$$

where $C_{S_l} = S_l / q_l A_i$

and A_i is defined on Figure A-3.

The empirical "efficiency factor" e_b provides a means for evaluating various shapes (such as those of Figure A-3) relative to the elliptic shape (see, for example, Wood [1955] Chapter 9). The calculation of drag due to sideforce in the case of the boards should include effects of "sidewash" of the body and "slot" effects at the daggerboard well (see, for example, Wood [1955], Chapter 14). In the present case, these were neglected.

Wherever lateral trim is a consideration (Letcher [1965]) the rudders will perform as sideforce producing surfaces with attendant induced drag. Air-water interface effects and ventilation (for example, Hoerner [1964] p. 11-29) become a consideration under these circumstances. In the present case, the rudders were assumed to operate at zero lift for all headings. Performance testing led to the conclusion that this is a reasonable approximation except when running with the main only (for the boat of the present investigation).

From previous considerations (equation (9))

$$S_h = R_a \cos(\beta - \delta_a) \tag{9}$$

which can be expressed in terms of coefficients by

$$C_{S_h} = \frac{\rho_a}{\rho_w} \frac{A_s}{A_i} C_{R_a} \cos(\beta - \delta_a) \left(\frac{V_a}{V_b}\right)^2 \tag{A-11}$$

and, substituting into A-10,

$$\left[\frac{C_{D_i}}{C_s}\right]_h = \frac{\rho_a}{\rho_w} \frac{A_s}{A_i} \frac{C_{R_a} \cos(\beta - \delta_a)}{\pi A e_b} \left[\frac{V_a}{V_b}\right]^2 \tag{A-12}$$

for streamlined shapes. Clearly, the hydrodynamic induced drag to sideforce ratio is not constant. It is a function of the variables $C_{R_a}(\beta)$, $\cos[\beta - \delta_a(\beta)]$, $[V_a/V_b]$; ie, to this approximation $[C_{D_i}/C_{S_h}]$ is a function of the aerodynamic wind angle β, the velocity ratio $[V_b/V_a]$, and quantities which are parameters in the problem. The statement that C_{R_a} and δ_a depend only on β will be justified in the following section.

The hydrodynamic lift required is greatest for the close hauled condition for a given value of true wind. Therefore, the maximum value of drag due to lift should occur at this heading. This may be seen by equation (A-12) from which may be formed the ratio

$$\frac{(D_i/S_{\ell})}{(D_i/S_{\ell})_{\substack{\text{close}\\\text{hauled}}}} = \frac{C_{R_a}\cos(\beta-\varepsilon_a)\left[V_a/V_b\right]^2}{\left[C_{R_a}\cos(\beta-\varepsilon_a)\left[V_a/V_b\right]^2\right]_{\substack{\text{close}\\\text{hauled}}}} \qquad \text{(A-13)}$$

For illustration, this was calculated for the boat of the present investigation using measured values of $\left[V_a/V_b\right]$ at different headings.

The foregoing discussion applies to streamlined sections as was previously stated. For the present investigation, stock DC - 14 boards were used for most of the runs. The section and planform are shown on Figure A-3. It was concluded that the lift and drag characteristics of such a configuration would be more nearly approximated by flat plate data than by lifting line theory. Therefore, an empirical equation describing the dependence of drag on lift was fitted to NACA data (Bruce [1962 b]). It results that

$$\frac{C_{Di}}{C_{S_{\ell}}} = 0.321\, C_{S_{\ell}}^{3/2} \qquad \text{(A-14)}$$

for the rectangular flat plate of $AR = 5$. Assuming $C_{R_a} = C_{R_{a_{max}}} \cong 1.5$; ($\beta = 30°$; $\varepsilon_a = \psi_a\big]_{C_{R_a}=1.5}$; and $(Va/Vb) = 2$; correspondingly,

$$C_{S_{\ell}}\Big]_{max} = 0.447 \qquad \text{(A-15)}$$

and the leeway angle is

$$\psi_{sh}\Big]_{max} = 8.5^{\circ} \qquad \text{(A-16)}$$

which is well above the 6° attack angle for minimum drag to lift ratio of the board. The maximum induced drag to sideforce ratio is

$$\frac{C_{Di}}{C_{sh}}\Big]_{max} = .09 \qquad \text{(A-17)}$$

according to this estimate. However, for a streamlined section of the same planform and aspect ratio and the same conditions,

$$\frac{C_{Di}}{C_{sh}}\Big]_{max} = 0.035 \qquad \text{(A-18)}$$

from equation (A-12) at an angle of yaw (leeway) of 7° which is doubly advantageous.

In summary, it is well known that the induced drag to sideforce ratio varies with heading to the apparent wind. A measure of the nature and degree of its dependence on heading for a boat trimmed for zero helm on all headings can be obtained from Figure A-4. An explicit expression of its dependence on β and $[V_b/V_a]$ is given by equation (A-12). Equation (A-12) when combined with equation (13), page A-1, yields equation (16), page 16, the performance equation in terms of the apparent speed ratio.

LIST OF FIGURES

TABLE I

GEOMETRIC PARAMETERS OF DC - 14 P

Ab	board total wetted area = 4.5 ft.^{2};
Af	(equation A-2) = [40.5 + .04 (crew weight)], ft.^{2};
Ai	"induced drag area" = 3.44 ft.^{2}
Aj	jib area = 40 ft.^{2};
Am	mainsail area = 100 ft.^{2};
Arud	rudder total wetted area = 4 ft.^{2};
Aspin	spinnaker area = 115 ft.^{2};
AR_b	board aspect ratio reflected (Fig. A-3) = 5;
AR_{rud}	rudder aspect ratio reflected (Fig. A-3) = 4.5;
k_s	hydrodynamic roughness = .002 inches;
	characteristic hull length (page A-3) = 12.5 ft.;
Wb	boat weight (sans crew) rigged for racing = 430 lbs.

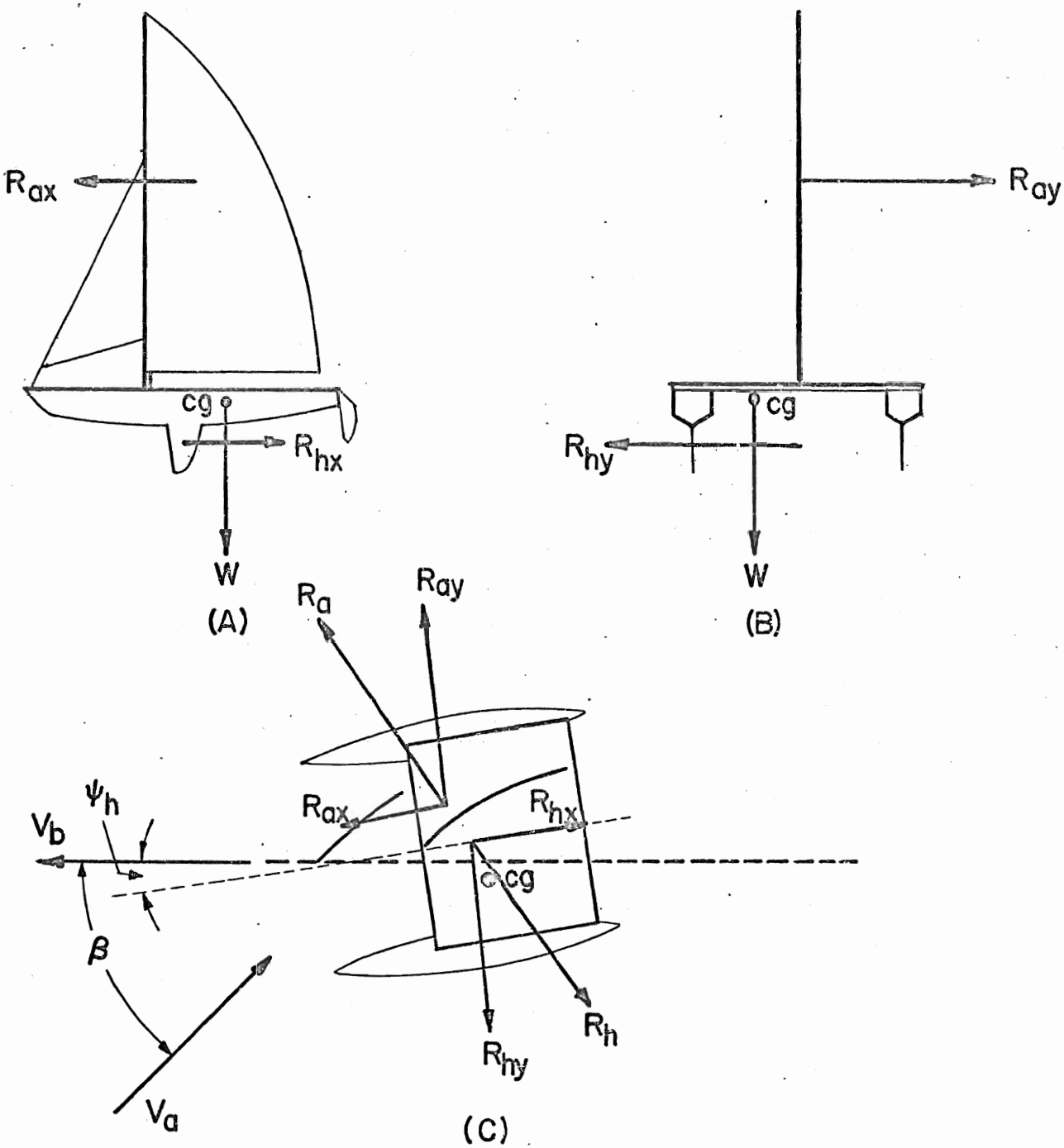

1. Resultant Force Components for the Simplified Problem.

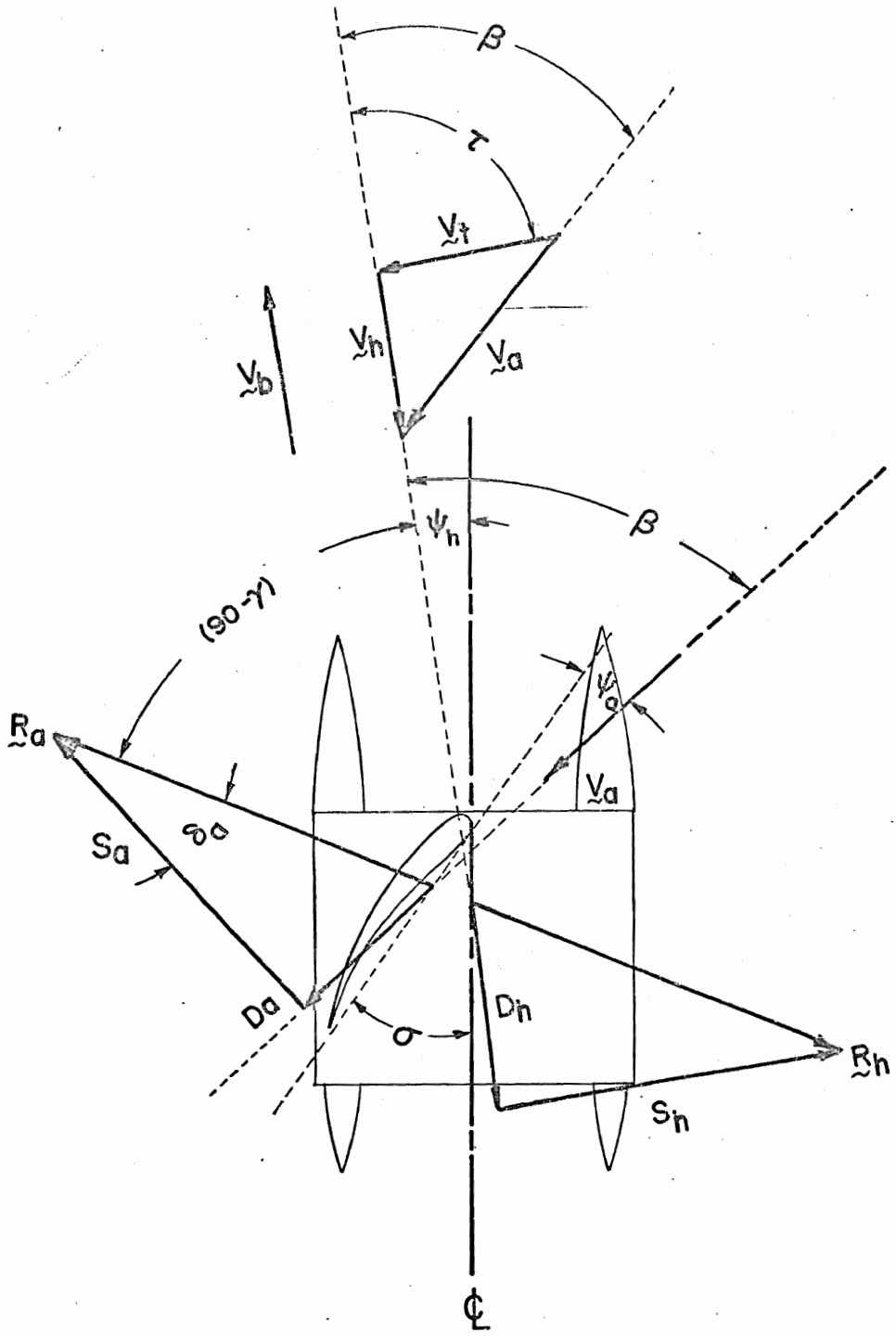

2. Definition of Terms in Body Fixed "Wind Axes".

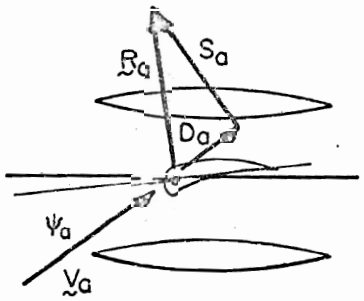

(a) Close Hauled

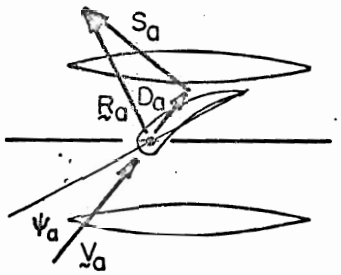

(b) Close Reaching

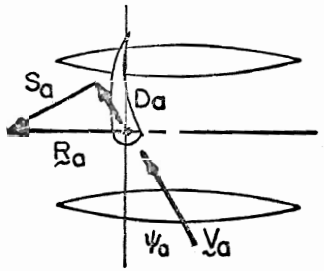

(c) Beam Reach

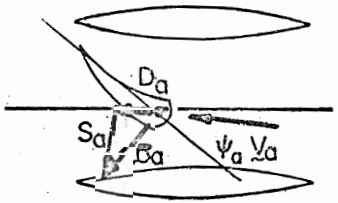

(d) Broad Reaching

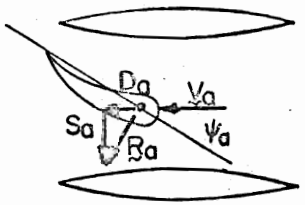

(e) Dead Run

3. Operation of the Idealized Unirig.

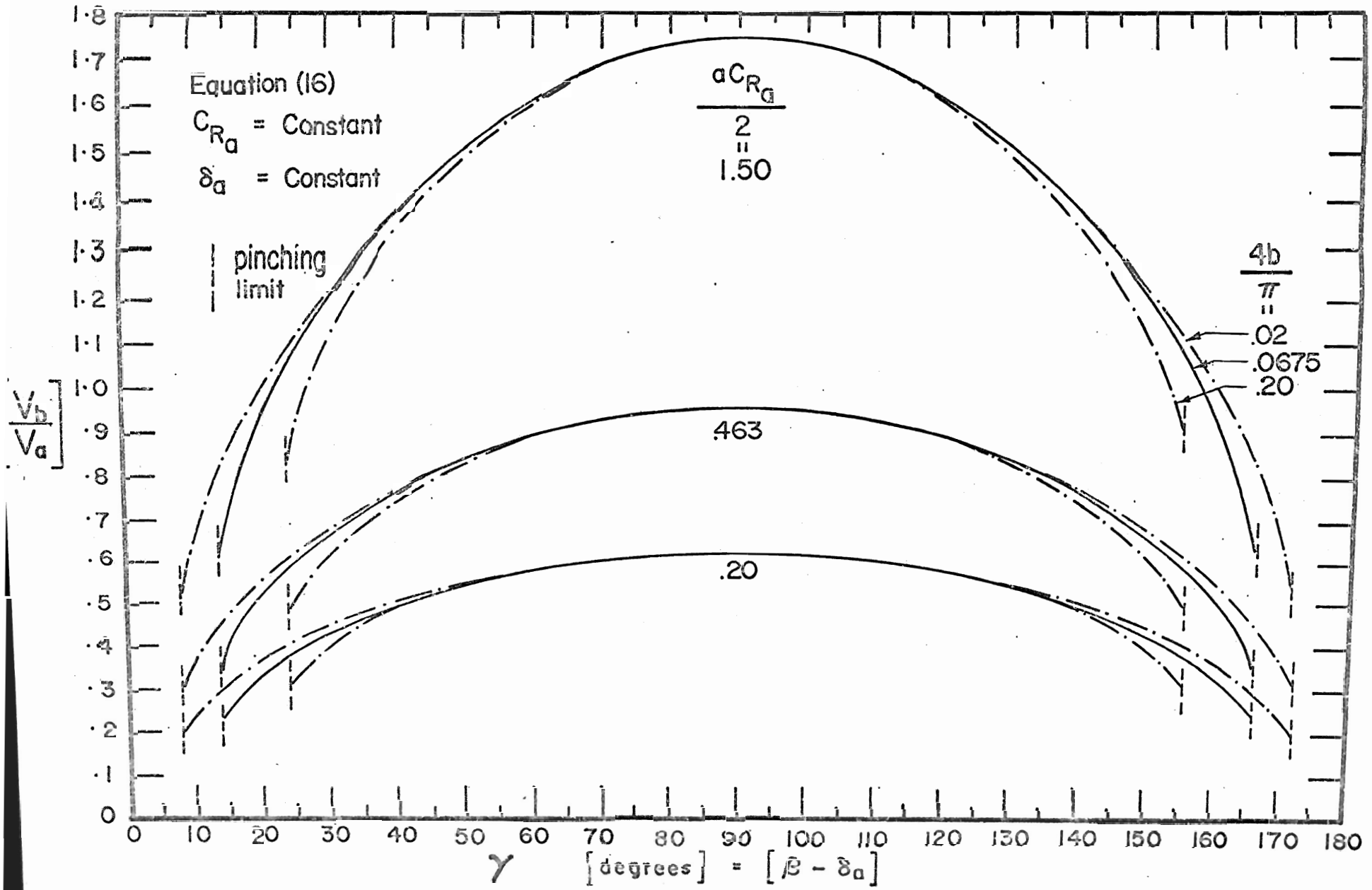

4. Apparent Speed Ratio as a Function of the Reduced Apparent Wind Angle (idealized unirig).

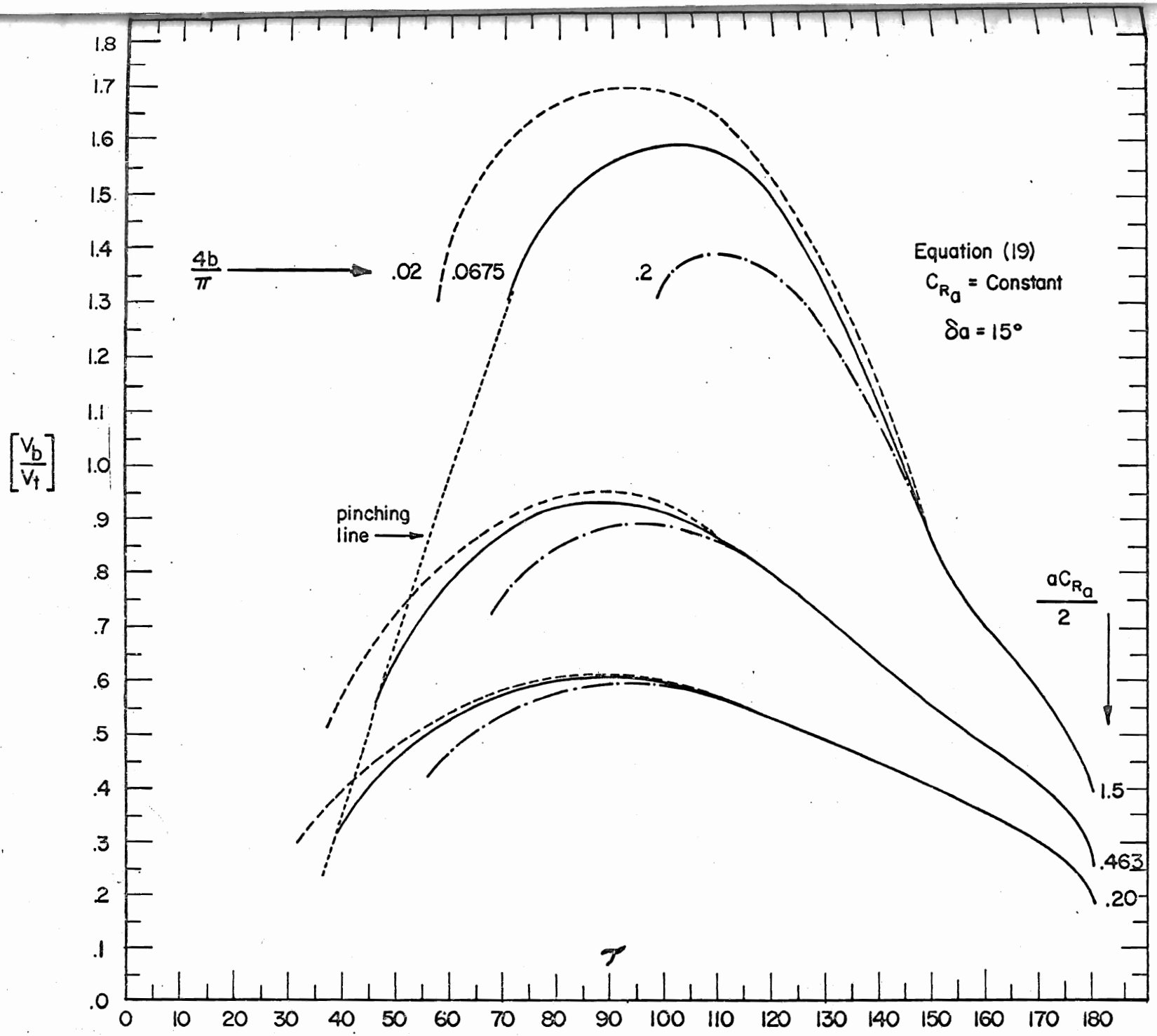

5. True Speed Ratio as a Function of the True Wind Angle (idealized unirig).

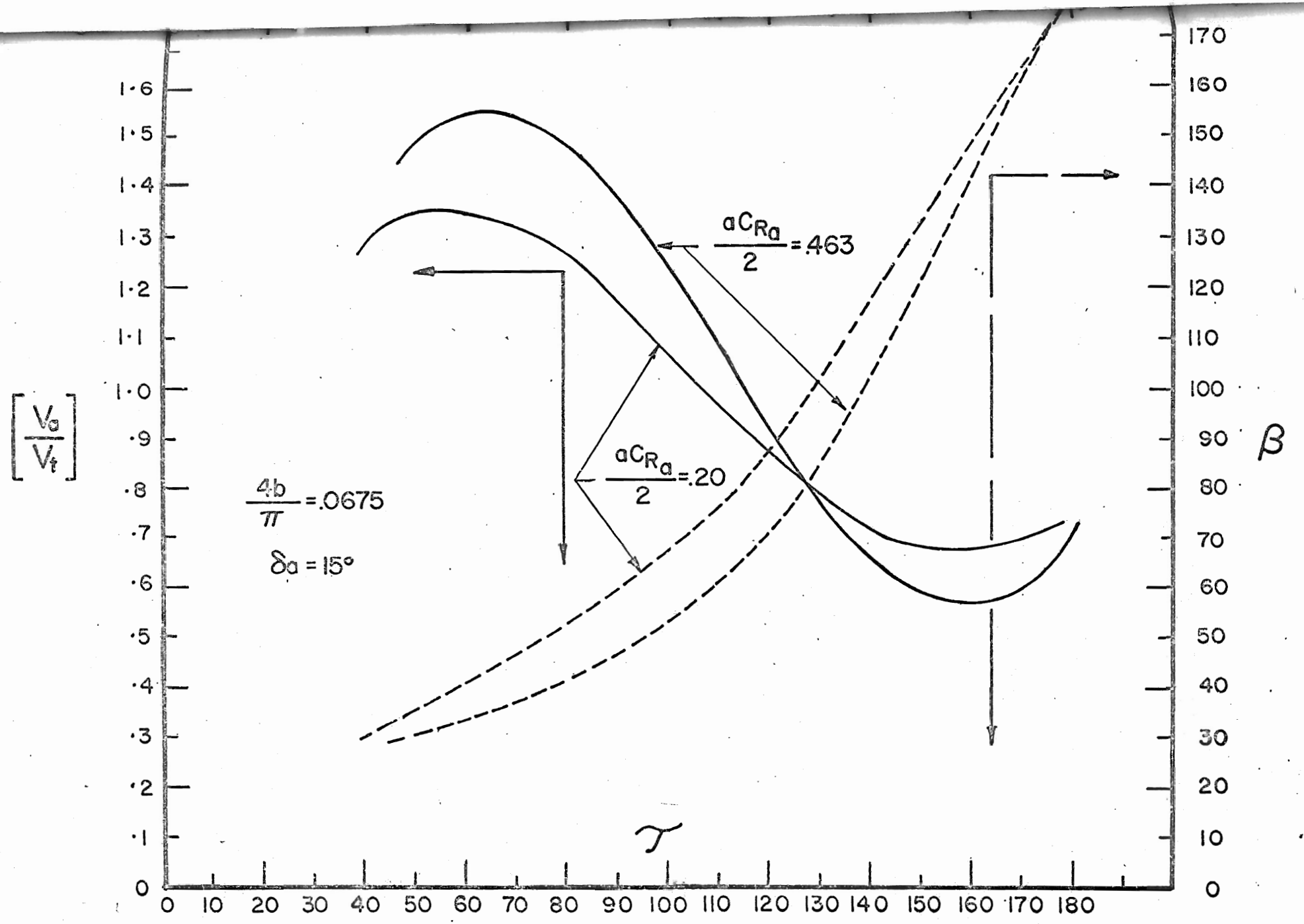

6. Apparent to True Wind Speed Ratio vs. True Wind Direction. Apparent Wind Direction vs. True Wind Direction (idealized unirig).

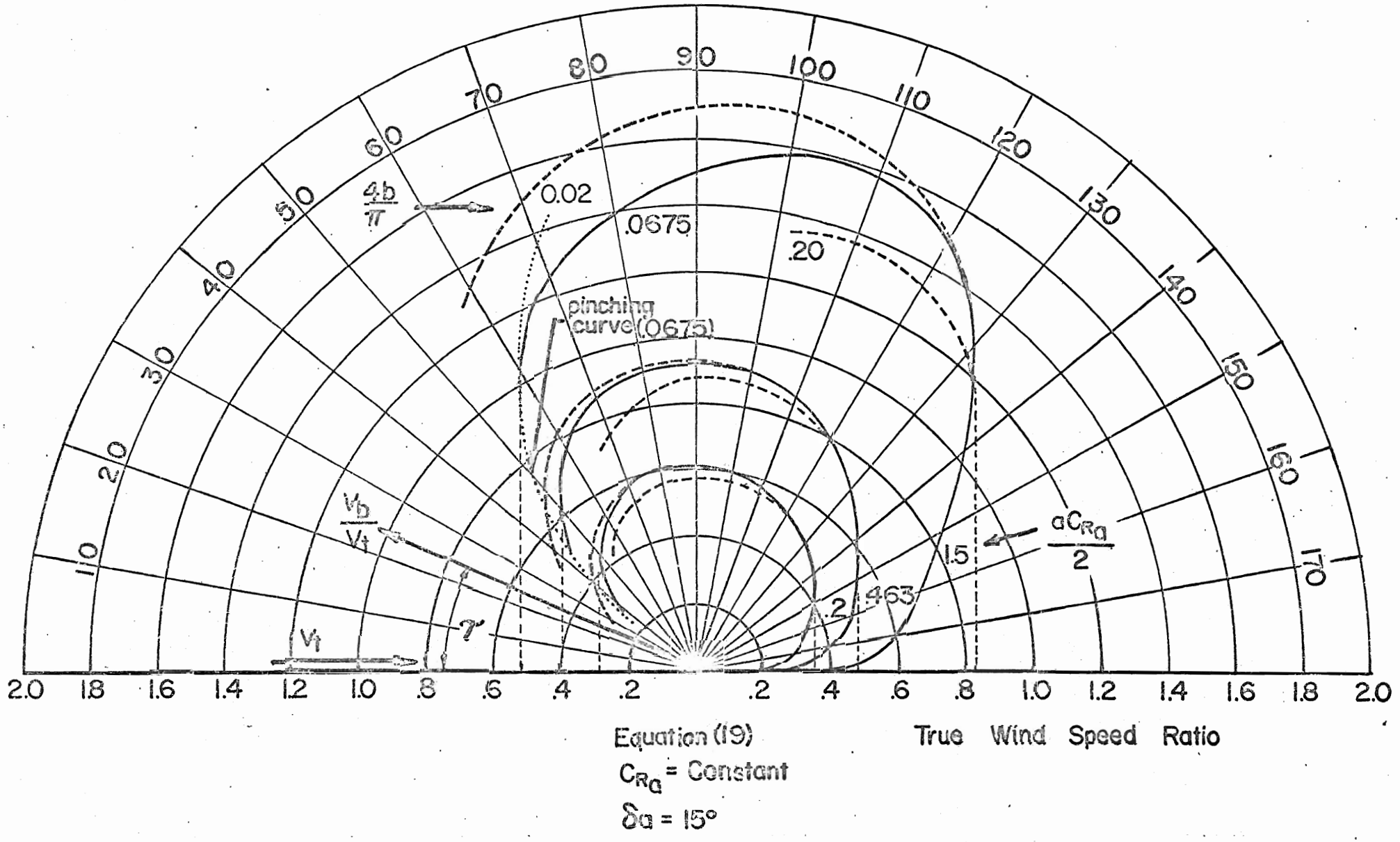

7. Performance Polar (idealized unirig) as Affected by Variations of Thrust Index and Hydrodynamic Drag Product.

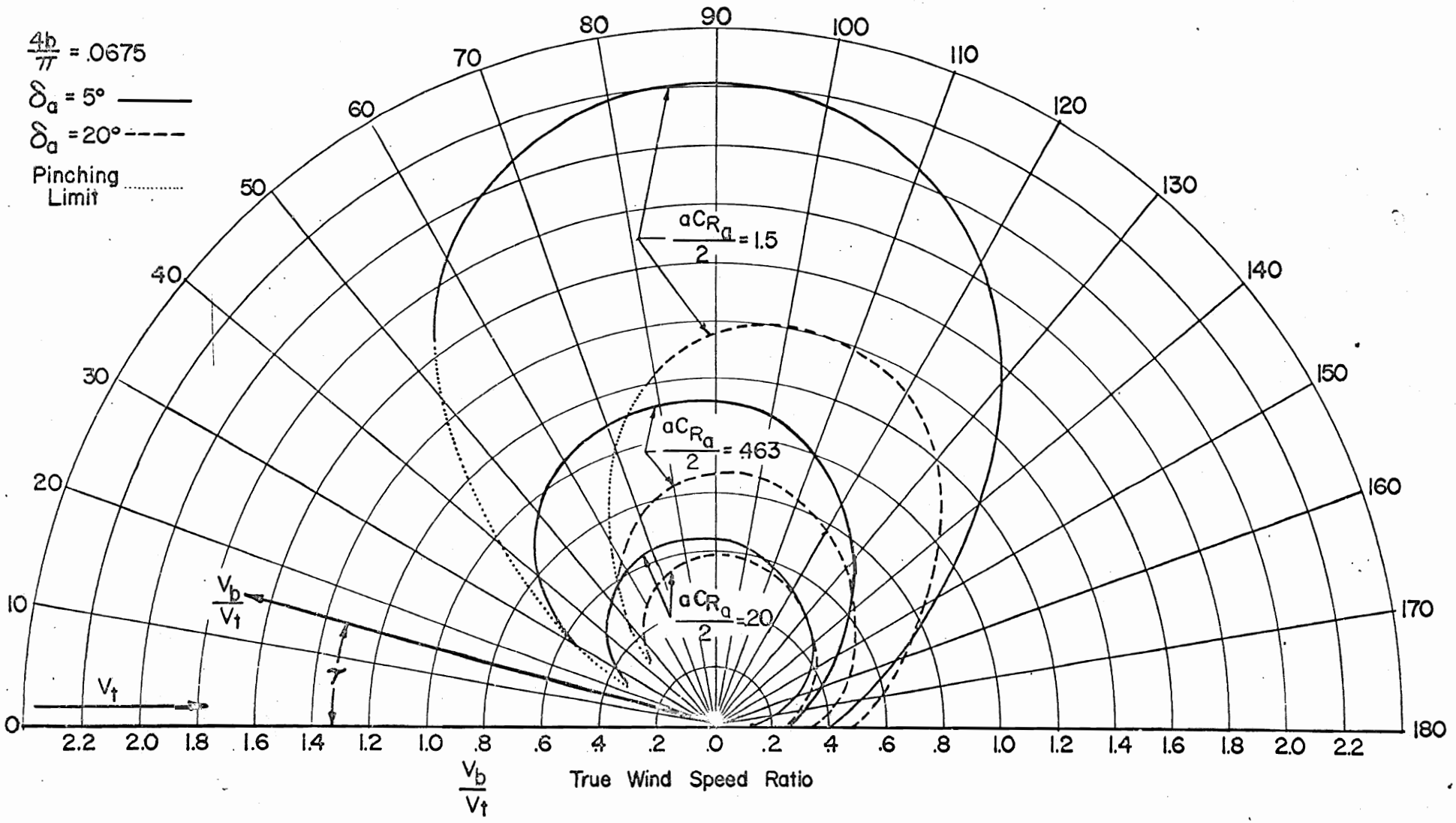

8. Performance Polar (idealized unirig) as Affected by Variations of Aerodynamic Drag Angle.

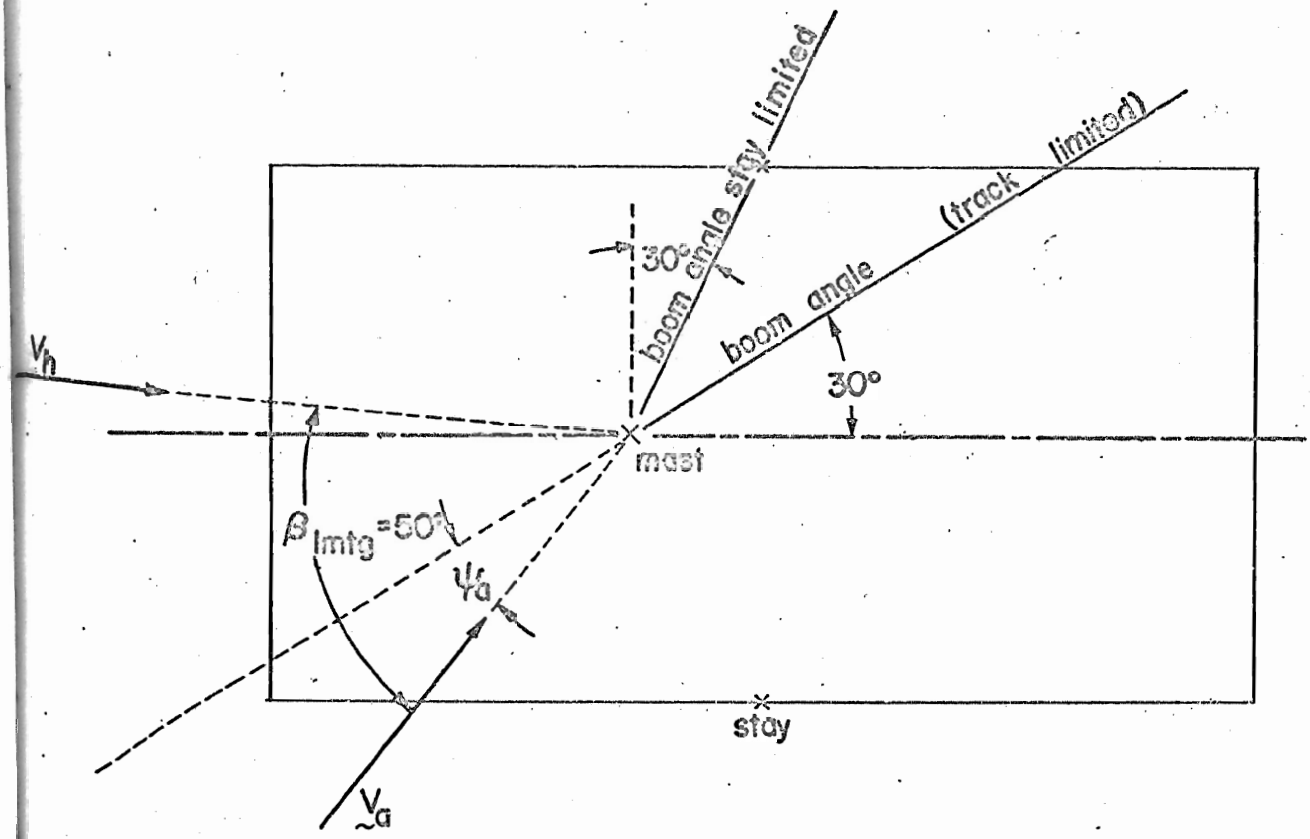

(a) Postulated Geometry

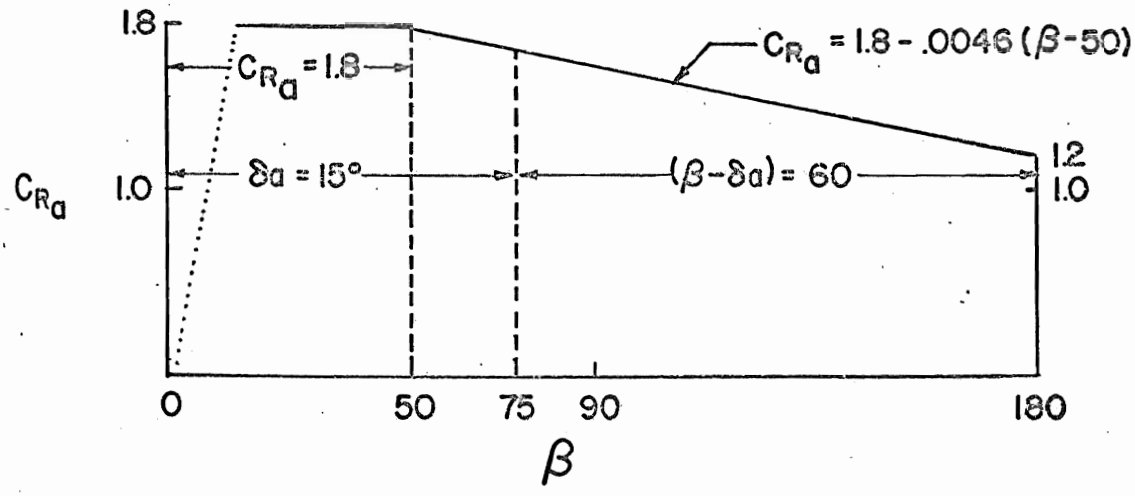

(b) Postulated $C_{R_a}(\beta)$

9. The "Stay Limited" Unirig. a) Postulated Geometry; b) Postulated $C_{R_a}(\beta)$.

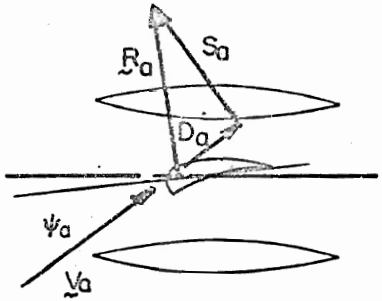

(a)

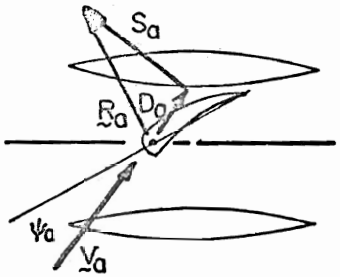

(b)

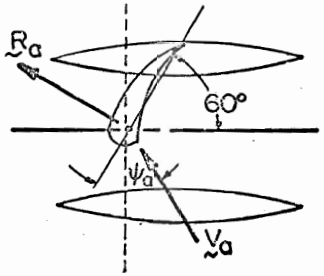

(c)

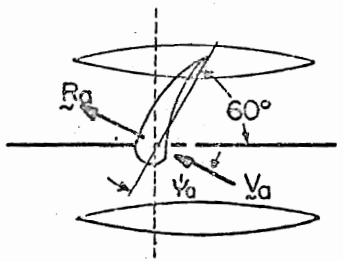

(d)

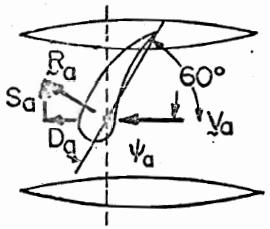

(e)

10. Operation of the Stay Limited Unirig.

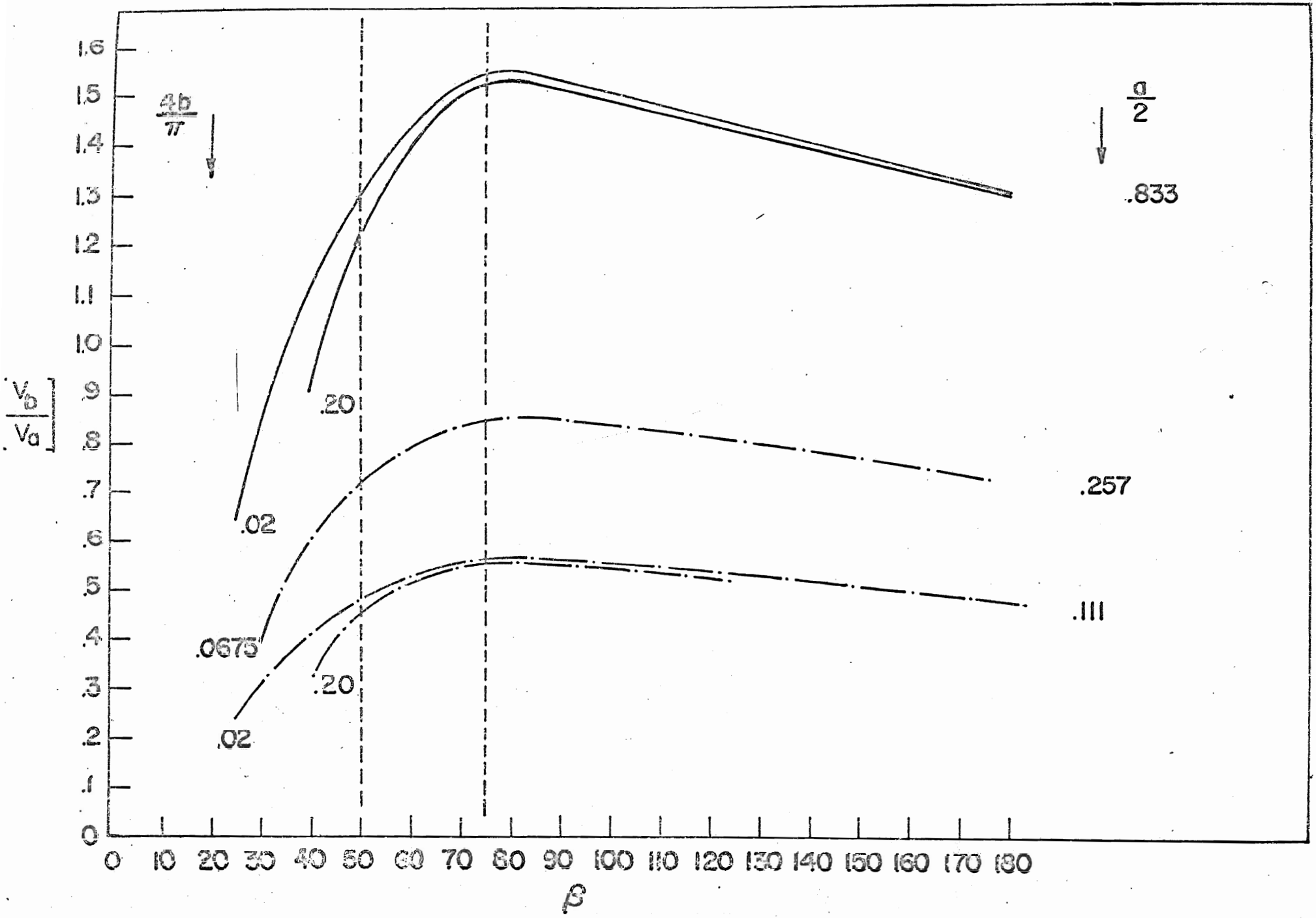

11. Apparent Speed Ratio as a Function of the Apparent Wind Angle (stay limited unirig).

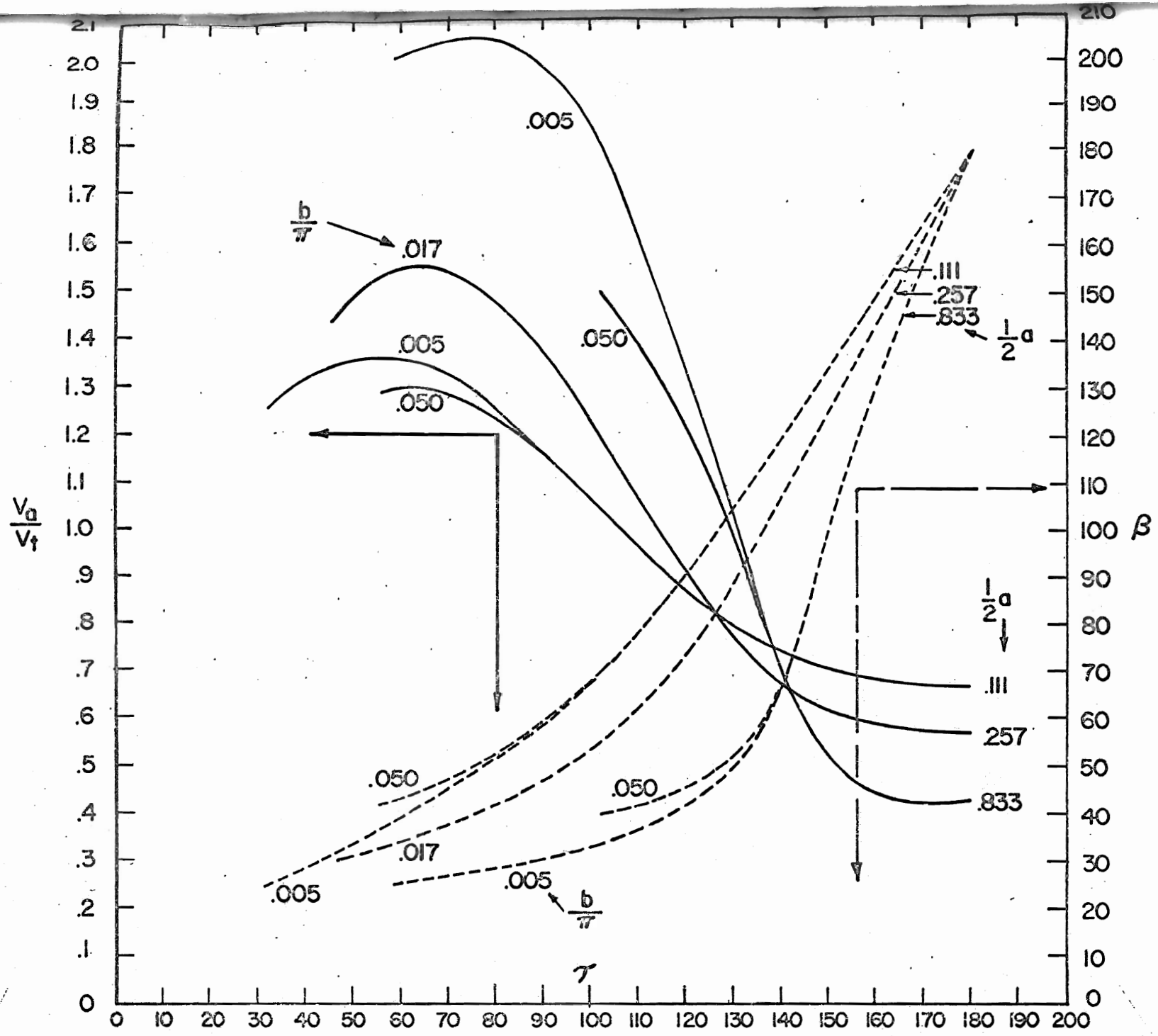

12. Apparent to True Wind Speed Ratio vs. True Wind Direction. Apparent Wind Direction vs. True Wind Direction (stay limited unirig).

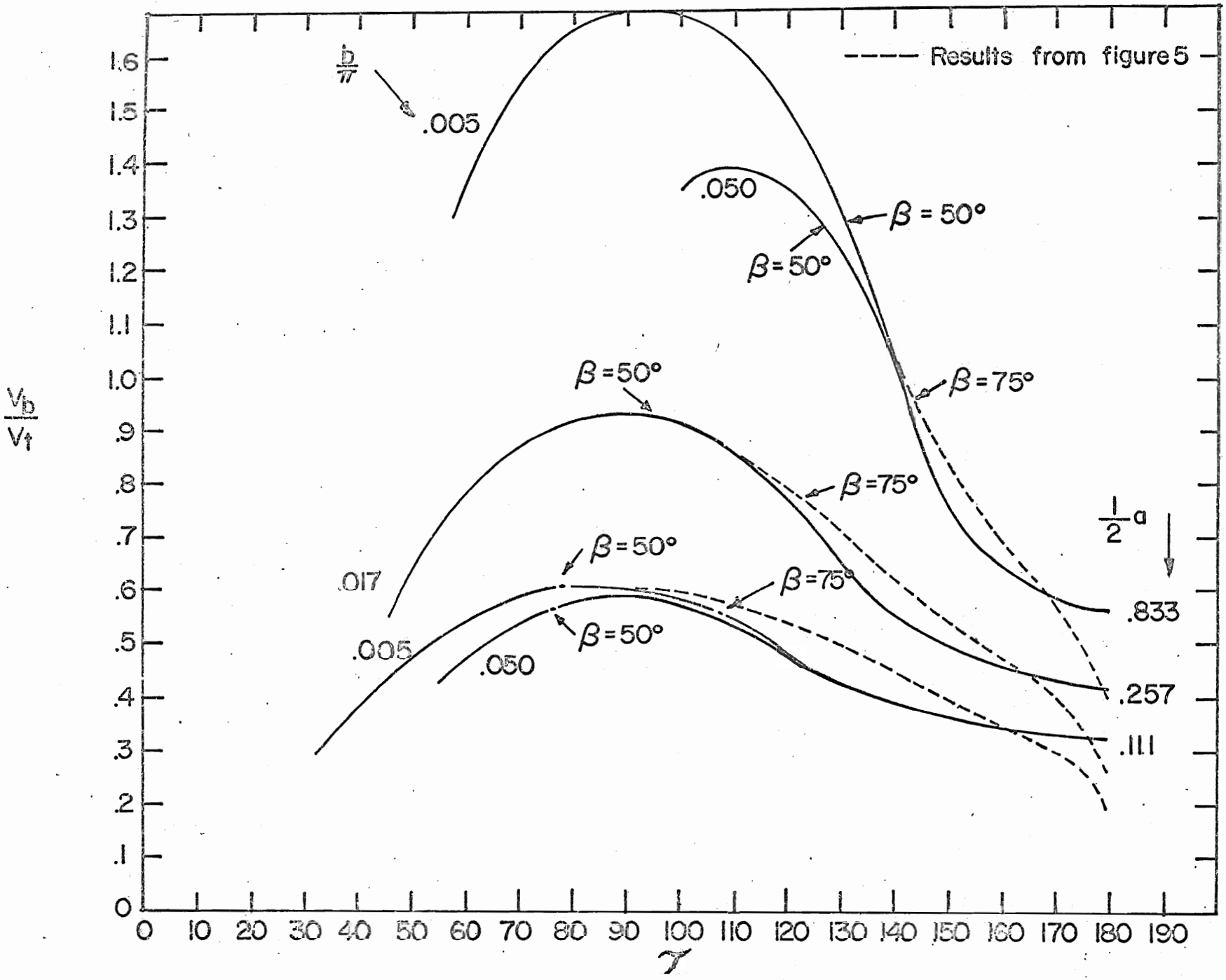

13. True Speed Ratio vs. True Wind Angle (stay limited unirig).

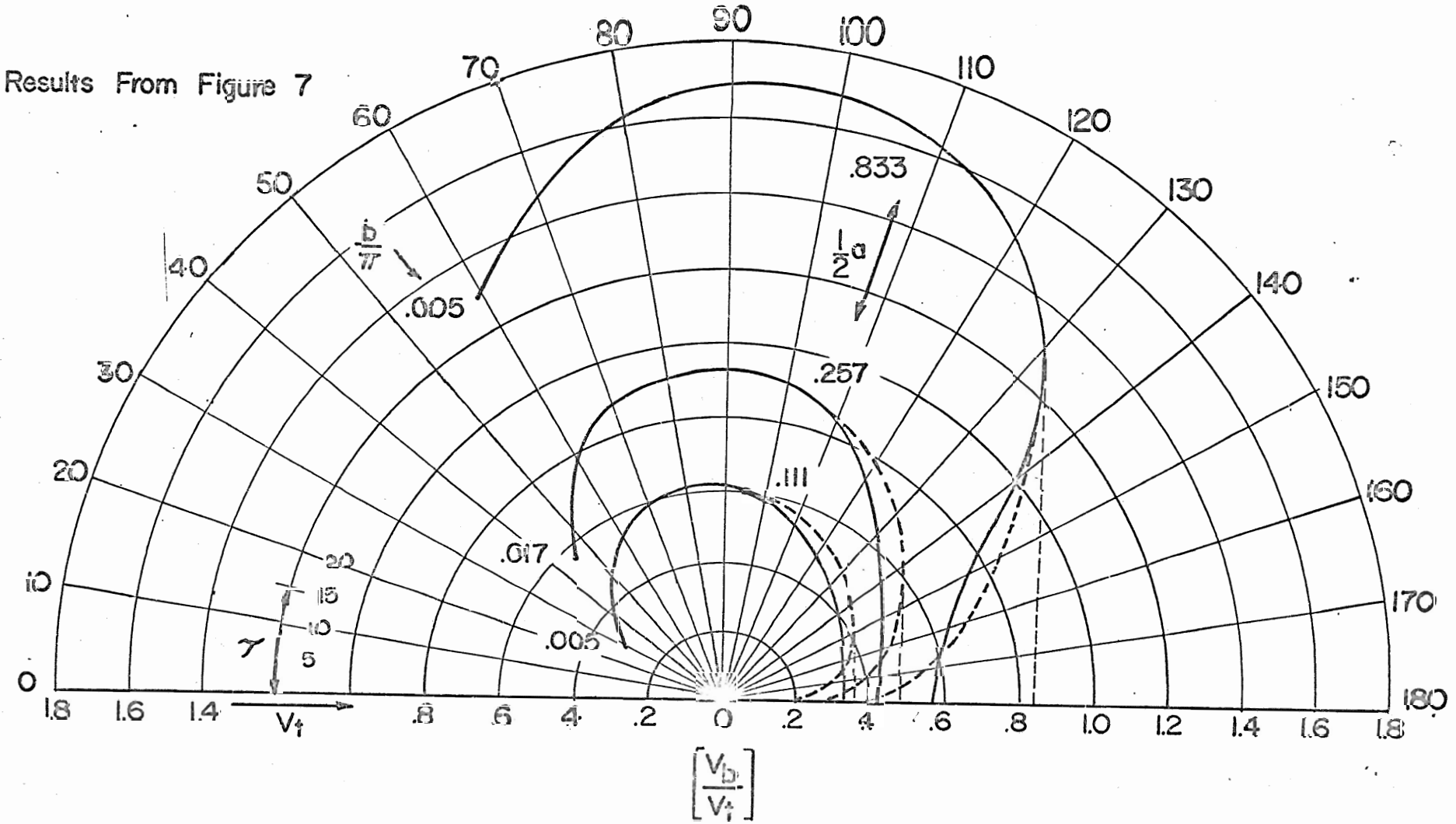

14. Performance Polar (stay limited unirig) as Affected by Variations of Thrust Index and Hydrodynamic Drag Product.

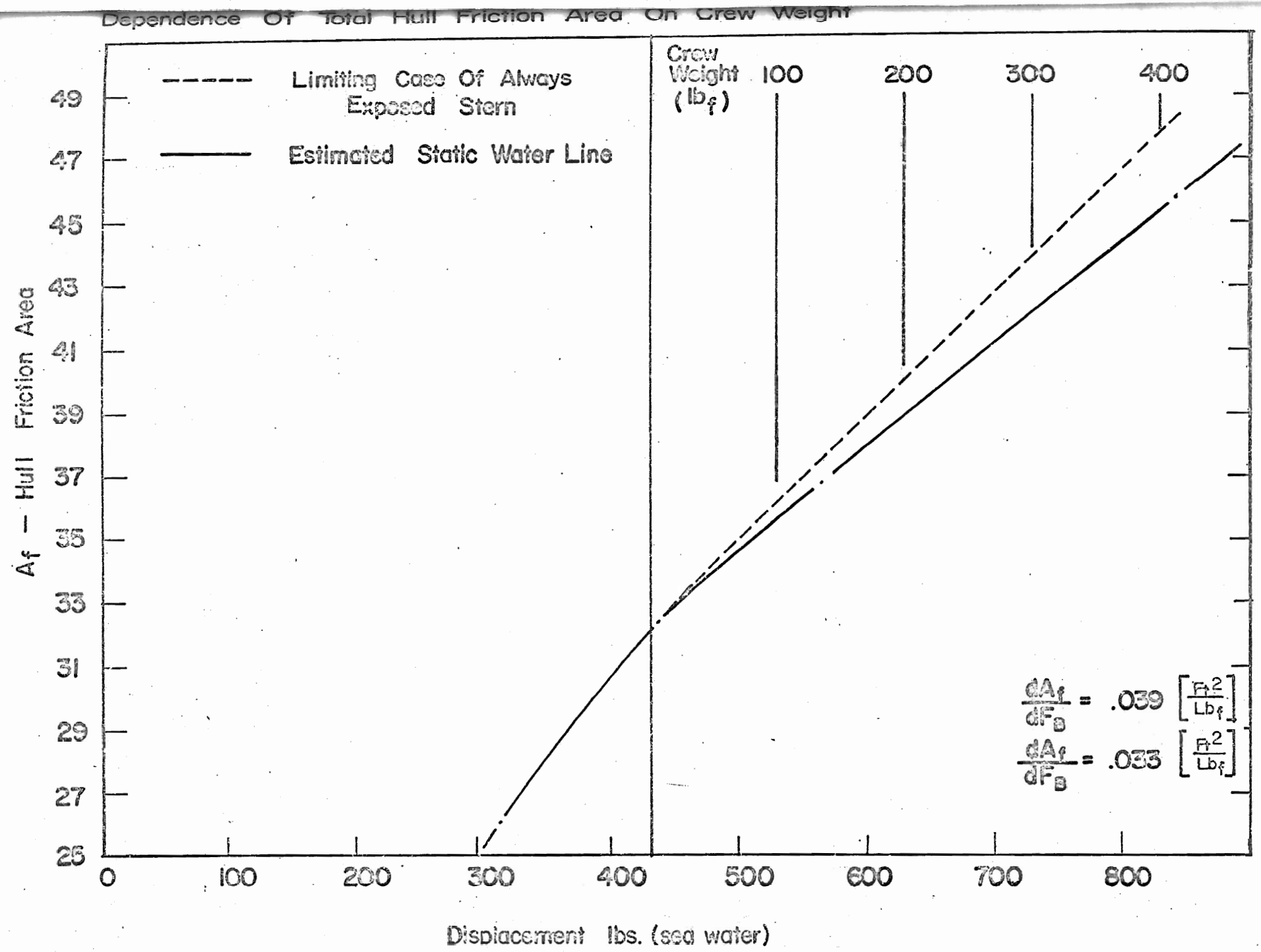

A-1. Dependent of Total Hull Wetted Area on Crew Weight (DC14 - P catamaran).

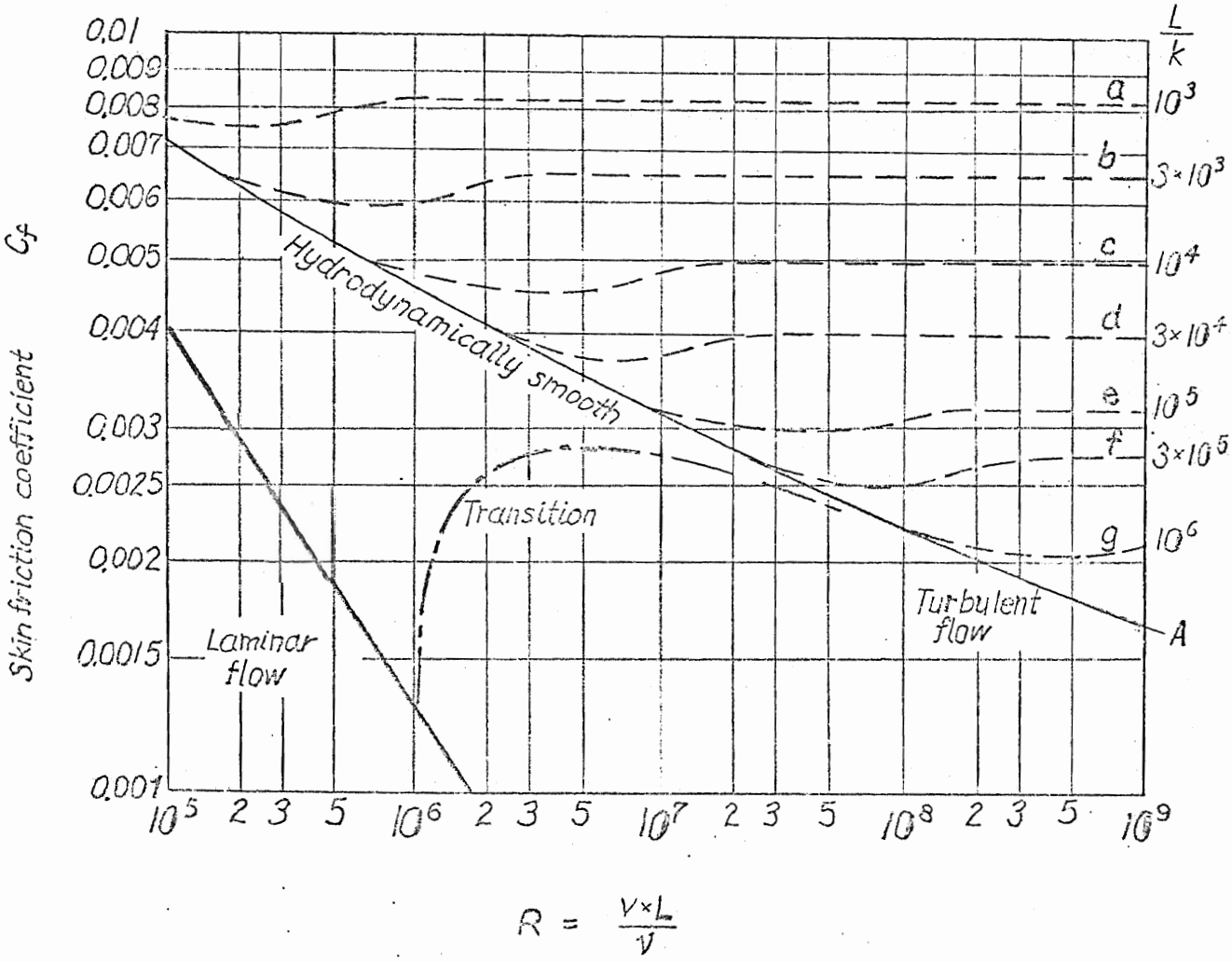

A-2. Skin Friction Coefficient vs. Reynolds' Number for Parameters of Surface Roughness.

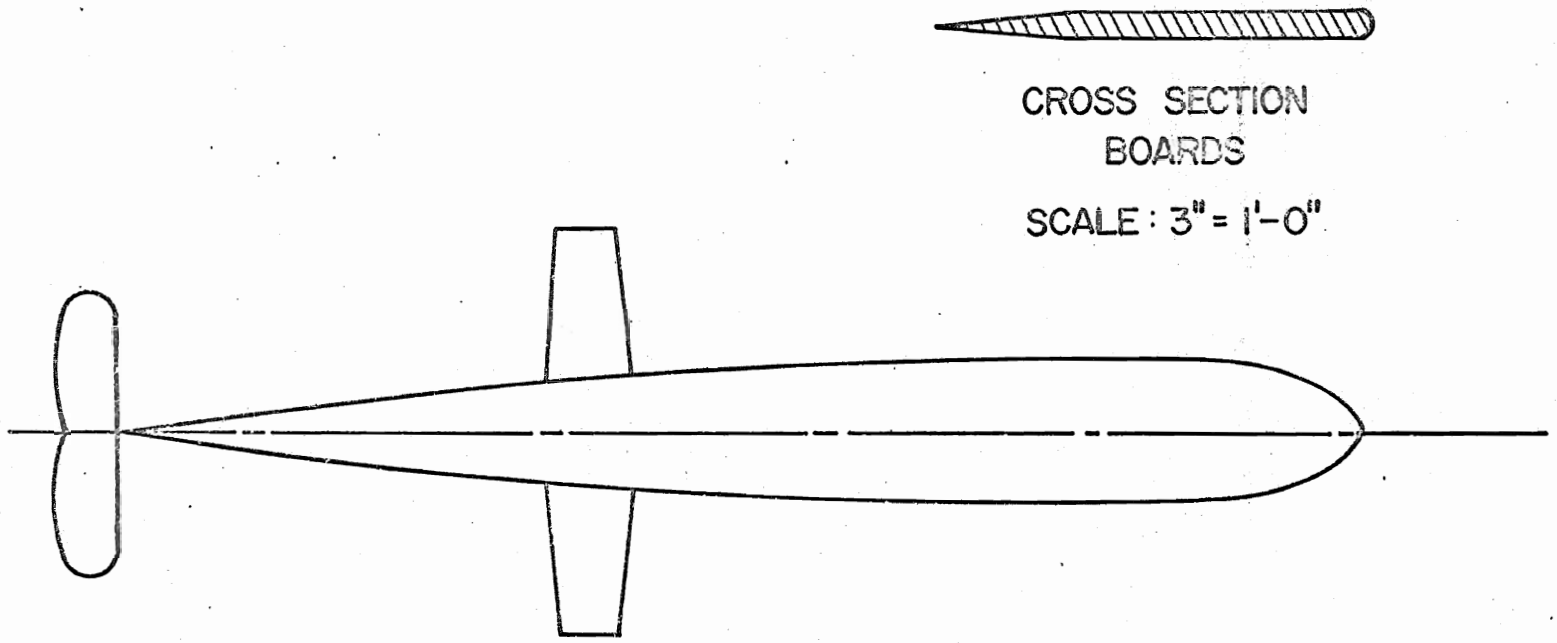

A-3. Hydrodynamic Reflection of DC14 - P Underbody.